CHARACTERISATION OF AND NICKEL EXTRACTION FROM LATERITES OF SUKINDA, ORISSA

by

VIJAYANAND SHARMA

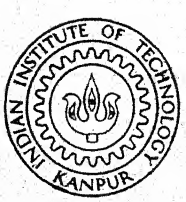

DEPARTMENT OF METALLURGICAL ENGINEERING
INDIAN INSTITUTE OF TECHNOLOGY KANPUR
MARCH, 1979

CHARACTERISATION OF AND NICKEL EXTRACTION FROM LATERITES OF SUKINDA, ORISSA

A Thesis Submitted
in Partial Fulfilment of the Requirements
for the Degree of

MASTER OF TECHNOLOGY

by

VIJAYANAND SHARMA

to the

DEPARTMENT OF METALLURGICAL ENGINEERING
INDIAN INSTITUTE OF TECHNOLOGY KANPUR
MARCH, 1979

In the loving memory of

my parents

(Late) Smt. DHANWANTI DEVI

&

(Late) Sri RAMESH CHANDRA SINHA

CERTIFICATE

This is to certify that the work 'Characterisation of and Nickel Extraction from Laterites of Sukinda, Orissa' has been carried out by Sri Vijayanand Sharma under my supervision and that it has not been submitted elsewhere for a degree.

S. Chander

(S. Chander)
Assistant Professor
Department of Metallurgical Engineering
IIT Kanpur

March 1979

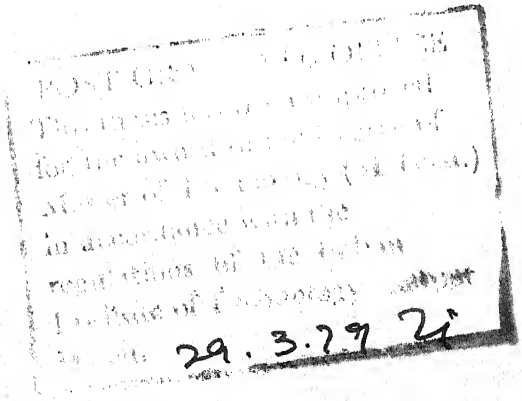

ACKNOWLEDGEMENTS

The author expresses his sincere gratitude to Dr. S. Chander for suggesting the problem, supervising the work, giving him encouragement and having fruitful discussions during the course of the work.

He is also grateful to Professors K. P. Singh and A. Ghosh, the former and the present Head of the Department of Metallurgical Engineering, IIT Kanpur respectively for releasing him from his duties to pursue the academic program and also for permitting him to use various facilities and equipments in their laboratories.

He also acknowledges and appreciates the help rendered by Dr. K. N. Rai of the Department of Metallurgical Engineering and Materials Science, IIT Kanpur in Transmission Electron Microscopic studies and for sparing his valuable time for discussing the results of the Electron Diffraction.

The author is indeed indebted to

(i) Professor D. W. Fuerstenau of the Department of Materials Science and Mineral Engineering, University of California, Berkeley for his assistance in Scanning Electron Microscopy and ESCA studies and in determining pore size and pore size distributions.

(ii) Dr. K. N. Han of Monash University, Australia for his help in DTA/TGA studies.

(iii) Dr. A. C. Shipstone of CDRI, Lucknow for permitting him to use the Scanning Electron Microscope and to members of his staff for their general assistance and co-operation.

(iv) Sri A. P. Raju of Bharat Electronics Laboratory, Bangalore for his help in the surface area measurements.

(v) Members of the faculty of the Department of Metallurgical Engineering who helped him in various ways and to members of staff of the Department of Metallurgical Engineering and various facilities who came to the assistance of the author in times of need.

(vi) Sri Nihal Ahmad, Sri R. K. Bajpai and Sri Triveni Tewari for getting the present work to a beautiful completion.

The financial assistance provided by the Department of Science and Technology, Government of India, New Delhi, to carry out this work, is gratefully acknowledged.

CONTENTS

LIST OF TABLES

LIST OF FIGURES

SYNOPSIS

The nickeliferous laterite ore from Sukinda, Orissa, has been characterised by various physical and chemical methods such as X-ray and Electron Diffraction, DTA, ESCA and Electron Microscopy. The ore was found to be a weak agglomerate of very fine particles with very high porosity and complex structure. It contained a mixture of poorly crystallized goethite with Fe(III) dominating and an amorphous gel containing Fe(II) which appears to be present on the surface of the particles as seen by ESCA studies. Nickel is uniformly and finely distributed throughout the ore body.

The extraction of nickel was found to be very sensitive to the phase changes during reduction roasting. Higher roasting temperature yielded more nickel with still higher iron than those at lower roasting temperatures. The reduced ore contained several iron rich phases in which the dissolution order was $FeO > Fe > Fe_3O_4$. The rate of extraction of nickel decreased with increase in roasting temperature although the total amount of nickel extracted is greater for higher roasting temperature. Cooling gas in combination with cooling time was observed to have played a major role in the extraction. Inert cooling gas gave the best results with a critical cooling period to cool the

sample to about 50°C. The 60/40 (v/v) mixture of H_2-H_2O was observed to give the best extraction of nickel at relatively small solubilization of iron. Larger amount of H_2 gave increase in iron dissolution without affecting nickel recovery. Addition of salts during roasting resulted in maximum nickel extraction at one percent for NaCl and $CaCl_2$ and at four percent for $MgCl_2$. The salt additions generally increased solubilization of iron. Phase changes during leaching indicated that dissolution of Fe_3O_4 was very slow and since Fe_3O_4 is formed at lower temperatures sintering effect is minimised and rate of extraction is higher. Hence formation of Ni and Fe_3O_4 seem to be the optimal condition for extraction of nickel.

CHAPTER 1

INTRODUCTION

At present about 75 percent Nickel is produced from the sulphide and remaining from the oxide and silicate ores. The oxide and silicate ore reserves, however, constitute about 75 percent of the nickel mineral, the remainder being sulphide ores. The developments in the technology for nickel production must, therefore, be focussed on treatment of the oxide and silicate ores. Richer oxide and silicate ores containing nickel greater than about 2.5 per cent have been treated by pyrometallurgical methods. This thesis concerns, however, with lower grade which requires processing either by a combination of pyrometallurgical and hydrometallurgical techniques or by hydrometallurgical methods. The reduction roasting - ammonia leaching as followed in Nicaro is an example of the Roast-Leach process. Purely hydrometallurgical route, using high pressure-high temperature sulphuric acid leaching is followed in Moa Bay. The literature on extraction methods using these techniques is reviewed in Chapter 2.

India does not have sulphide or rich oxide ores of Nickel but has a reserve of about 65 million tons of laterite

ore in Sukinda, Orissa containing about 1.3 percent nickel. This being a low grade and complex ore, it is very difficult to beneficiate the ore by physical or pyrometallurgical methods. The present investigation, sponsored by the Department of Science and Technology, Government of India, New Delhi, is to study the ore characteristics and to establish the extraction behaviour of nickel by the reduction roast-ammonia leach process.

The ore was characterised by the following techniques:

(i) Nickel analysis in different fractions of the dry and wet sieved ore.

(ii) surface area measurement

(iii) measurements of pore size and pore size distributions.

(iv) X-ray and electron diffraction.

(v) Scanning and transmission electron microscopy.

(vi) Differential Thermal and Thermogravimetric analysis, and

(vii) ESCA studies.

Chapter 4 deals with the effect of heat treatment in various reducing environments on the ore properties.

The effect of various roasting variables such as roasting temperature, H_2/H_2O ratio, salt additives, and cooling conditions on the leaching behaviour of the ore is discussed in Chapter 5.

CHAPTER 2

LITERATURE REVIEW

2.1 Nickeliferous Laterites

The nickel content of a lateritic ore is of the order of 0.8-2.5 percent. Typical analysis of some nickeliferous lateritic ores is given in Table 2.1. The ores are classified as limonitic if they contain nickel distributed primarily in iron oxides, and as serpentinic if the nickel is present in silicate or serpentine phase. The ore may contain high nickel-minerals, such as high nickel garnierite, distributed in gangue minerals or it may contain low nickel bearing minerals uniformly distributed through out the ore body. In the former case it would be desirable to expose the high nickel mineral by grinding so that it can react with suitable reagents during extraction process, whereas in the latter case extraction of nickel by hydrometallurgical processes may involve decomposition of the matrix containing the nickel mineral.

The nickeliferous laterite ores are known to contain nickel in several forms depending upon the conditions of laterisation during weathering of parent rock to form a given ore body. The nickel found in laterites are present either

TABLE 2.1. Chemical Composition of Some Nickeliferous Laterite Ores.

	Limonitic Laterite				Silicate Laterite		
	Sukinda	Cuba	Philippine	New Caledonia	Sukinda	Philippine	New Caledonia
Ni	1.25	1.24	1.20	1.40	0.80	1.48	2.27
Co	0.03	0.12	0.12	0.26	0.05	0.03	0.16
Fe	49.00	41.90	48.00	45.00	30.72	12.40	26.80
Mg	0.30	1.60	0.30	0.30	0.24	17.50	7.40
Cr	0.60	1.60	2.30	2.20	2.12	0.90	1.40
Mn	0.70	0.50	0.80	1.10	0.65	0.20	0.40
Al	1.90	1.80	3.50	2.20	2.38	1.30	0.90
SiO_2	9.50	10.60	2.00	9.20	39.38	32.40	21.40
Ref.	6	7	7	7	6	7	7

as simple compounds of nickel, e.g. hydroxides in Ni(II) or Ni(III) state as in a hydroxide of nickel and magnesium,[1] and carbonates, as cationic substitutions in other minerals or as high-nickel nodules. Cationic nickel substitutions have been found in limonites, ferromagnesian silicate minerals and clays. Combes[2] suggested that nickel is associated with goethite either as lattice ion or as an unidentified phase intimately mixed with goethite. Turner[3] and Roorda and Queneau[4] have suggested presence of manganiferous micronocules. Roorda et al. detected micronodule of 20-40μ diameter having an estimated composition of 20 percent each of Ni, Co and Mn in New Caledonian minerals. Machpherson and Livingstone[5] have found evidence for existence of nickel as NiOOH in ores of Unst, Shetland.

Laterization Process

A simplified definition of the laterization process, given by Holland in 1903, is the tropical weathering of aluminosilicates in which silica, alkalis and alkaline earths are removed and alumina and iron oxides remain behind. The actual process, which is somewhat more complex, depends upon temperature, time, climate proximity to sea as a source of inorganic salts, physiography, precipitation, rock structure, movement of water table, length of hydrologic cycle, topographic profile and the balance between micro and macrofluora, the

physiographic surface must be relatively stable and a warm climate with heavy but intermittent rainfall to be essential- rainfall providing water for weathering process. These conditions favour breakdown of silicates and lixivation of silica, alkalies and alkaline earths. Alternate wetting and drying facilitates laterization process.

Lixiviant, rainfall, picks up various reagents such as CO_2, O_2, N_2 and NaCl (near sea coasts). The proportion of oxygen dissolved in rain water is notably higher than that in the normal atmosphere. Tropical thunderstorms convert some of the oxygen to ozone and hydrogen peroxide, which are strong oxidising agents. Water carrying these reagents penetrates rock which is facilitated by warm climates. Formation of ammonia, methane and other organic acid may take place. Bacterial action is also favoured by warm climate. Additional carbon dioxide produced by the decomposition of organic matter also accompanies these reagents through the rock.

In aerated rocks above the water level, dissolution reactions occur in a film of lixiviant between mineral and air. The concentration of soluble constituents increase as dissolution proceeds until the next rainfall when the fill water is drained by the wash water. Below ground level water the reactions occur in a water bath which tends to maintain dilute solutions. There is no general agreement

among investigators as to whether the bulk of the reaction products are ionic or colloidal. Both ionic and colloidal reactions seem to occur. The reaction products may be transported to new sites as ions or colloidal particles.

The first element to dissolve during initial stages of laterization is magnesium, followed by hydrolysis of ferro silicic acid to form silicic acid, colloidal silica and iron hydroxide. In solutions with sufficient oxidizing power or high Eh because of dissolved oxygen or other oxidising agents, the dissolved Fe(II) immediately oxidises to Fe(III) and precipitates as $Fe(OH)_3$. Initially the precipitated ferric hydroxide is non-crystalline or in gel form which may transform to limonite containing goethite or lepidocrocite or hematite, maghmite etc. Precipitating gel tends to entrap colloidal particles enriched in Ni, Mn and Cr as found by Roorda and Queneau[4]. The nature of impurities, time and temperature of aging influence the crystallization process. Iron (III) can be transported only in colloidal form because of insolubility of ferric oxides and hydroxides under ambient conditions. Fe(II) ions can be transported to a soluble $FeCO_3$ only in complete absence of oxygen in solution, or more generally, only in reducing environment, i.e. low Eh. If large amounts of CO_2 are available transportation of iron as Fe(II) is more generally favourable. Presence of significant amount of humic acid is also an indicator of reducing environment.

The dissolved or colloidal silica is transported to other areas enriching Ni, Mn, Cr and Fe. Peptization of silica is aided by organic colloids or hydrochloric acid present in the lixiviant. Co(III) is also transported and is precipitated as the pH of the solution increases. Iron may also remain in ferrous state in a reducing environment and be transported upwards during evaporation cycle. This seems to be the situation at Matano, Columbia.[8] Perdigon are developed by accretion of iron and aluminium oxides moving upward by capillary action during periods of intense evaporation. These oxides precipitate as water evaporates.

Nickel may also migrate as chloride under strong oxidising conditions. Migrating nickel readily replaces magnesium in magnesium silicates. Part of nickel may also be scavanged by ferric hydroxide particles or gel. Laboratory attempts to make nickeliferous iron oxide have been so far unsuccessful, however.

Mineralogy of Sukinda Nickel Ore

Mineralization of nickeliferous lateritic ores in the Sukinda Valley, Cuttack, Orrisa, has been investigated by the Geological Survey of India,[9,10] Nickel occurs in two distinct zones underlying lateritic mantle. Upper zone is nickeliferous limonite and lower zone is serpentine. The nickeliferous limonitic ore contains goethite and smaller

amounts of hematite, magnetite, quartz and chromite. Nickel is believed to be predominantly associated with goethite and to a lesster extent with magnetite. Lower zone is serpentinic with earthy green appearance and brownish tinge due to limonitization. It contains nickeliferous montmorillonite, serpentine and goethite. Nickel ore zones are of 20 to 40 meters thickness with highly variable grade ranging from 0.5 to 2.0 percent Nickel.

Nickel in the limonitic ore could be present either as divalent cation substituted in goethite/limonite lattice or as a nickel mineral of unknown character finely distributed in iron oxides. In both cases, it would be essential to dissolve the iron mineral for recovery of nickel. Attempts to synthesize nickel substituted goethite have not been too successful although a Cu containing goethite has been reported to be synthesised.[11] Any method aimed at selective extraction of nickel would invariably involve changes in iron oxide. It is this aspect which makes extraction of nickel difficult. Although there is a possibility that nickel is present as ions adsorbed on the surface of iron oxides, attempts to extract it through ion exchange type of process have not been successful so far. Presence of higher oxidation states of Ni as NiO_2, Ni_2O_3 have not been considered much in the literature on laterites although Pigeaud[12] has observed their formation during anodic polarization of nickel.

2.2 Treatment of Nickeliferous Lateritic Ores

There are two general routes available for treatment of nickeliferous lateritic ores. Pyrometallurgical processes hav been used primarily for treatment of high grade and silicate ores to produce nickel mattes or ferronickel.[13] Hydro-metallurgical processes have been more commonly employed to process lower grade ores. Acid leaching involving high temperatures and high pressure and reduction roasting followed by leaching are two main processes used for extraction of nickel.[13] In the acid leaching processes H_2SO_4, HCl, H_2SO_3 and Cl_2 have been used to treat the ores without prereduction of the ore. High pressure sulphuric acid leaching is commercially used at Moa Bay.[13,14] Studies on the use of HCl for atmospheric and pressure leaching of laterite ores in preference to H_2SO_4, have suggested pressure leaching in HCl where problems with disposal of residue and solutions exist for leaching with H_2SO_4.[15] In HSO-HTCP[16,17] process the finely ground ore and sulphur are heated in a slurry at 230-240°C at high pressure to sulphidise the ore. Nickel sulphide changes to nickel sulphate but iron sulphide is oxidised to Fe_2O_3 in the oxidation stage. Chlorine leaching[18] has also been tried for limonitic ores to recover nickel but the process is not found selective as it also dissolves iron and corrodes the reaction vessels, though it gives relatively good extraction of nickel.

Alternatively, reduction roasting followed by leaching the reduced ore has been practiced to treat lateritic ores.[19-26] The process combines pyro- and hydro-metallurgical techniques to treat the ore. Some of the details of the reduction treatment and the conditions used for leaching by various investigators are given in Table 2.2. A simplified flowsheet of the process is also given in Figure 2.1. In general, limonitic ores require more carefully controlled conditions than low iron high magnesium/silica ores since in the latter there is less tendency for the iron oxide to be reduced to the metallic state.

Nicaro process based on Caron's studies[25] have been discussed in detail by Queneau[13] and Power and Geiger[27] in which the reduced ore is cooled in non-oxidising atmosphere and then leached in ammoniacal ammonium carbonate solution to extract nickel. The ammoniacal solutions containing nickel and cobalt are boiled to remove ammonia and precipitate nickel as a mixture of nickel carbonate and hydroxide which is calcined to give nickel oxide. In the Caron process the nickel oxide contains cobalt oxide as an impurity. Battelle Memorial Institute[28] and Sherrit Gordon[29] investigated the conditions for cobalt separation from nickel and produced a cobalt-free product. In Sherritt Gordon process the nickel and cobalt are separated by selectively precipitating nickel metal as powder by pressure reduction with hydrogen.

TABLE 2.2. Typical Data for Reduction and Leaching Conditions for Treatment of Lateritic Ore by Reduction Roast-Leaching Processes.

Ore Type	Reduction: Reducing agent	Reduction: Temperature, °C	Reduction: Additives, %	Leaching: Lixiviant	Leaching: Air/O_2 used	Leaching: Ni recovery, %	Leaching: Other recoveries, %	Remarks	Ref
Serpentine	H_2	500-900	-	H_2SO_4 (30°,50°, 70°C)	Air	83	17 Mg	At 700°C	19
Ni oxide ores	CO	380-750	FeS_2 (0.3-2)	AAS	Controlled O_2	90	-	2 stage leaching 1.2% Pyrite	20
Ni oxide ores	$CO+CO_2+SO_2$	650-800	2 NaCl	Dil. H_2SO_4	Oxidising	80	30 Fe and Mg	At 80°C Leaching	21
Limonite	CO	380-700	FeS_2 (0.3-2)	AAS	O_2	92	87 Co	1.2% FeS_2	22
Limonite	CO	350-600	FeS_2 (0.3-2)	AAS	O_2	90	83 Co	Multi stage leaching	23
Nickeliferous laterite + Garnierite (serpentine)	High S coal	650-750	High S coal (3) $+FeS_2$(5)	AAC	O_2	88	5 Fe	-	24
Limonite + serpentine	H_2+H_2O/ $CO+CO_2$	650-950	FeS_2 NaCl $CaCl_2$	AAC	O_2	97	-		25
				Aq. $CuSO_4$ soln.		99	-		25
Laterite	$CO+CO_2$	700	-	Aq. $CuSO_4$ (pH 2.0)	-	87	-	In ½ hr	26

AAS : Ammoniacal Ammonium Sulphate.
AAC : Ammoniacal Ammonium Carbonate.

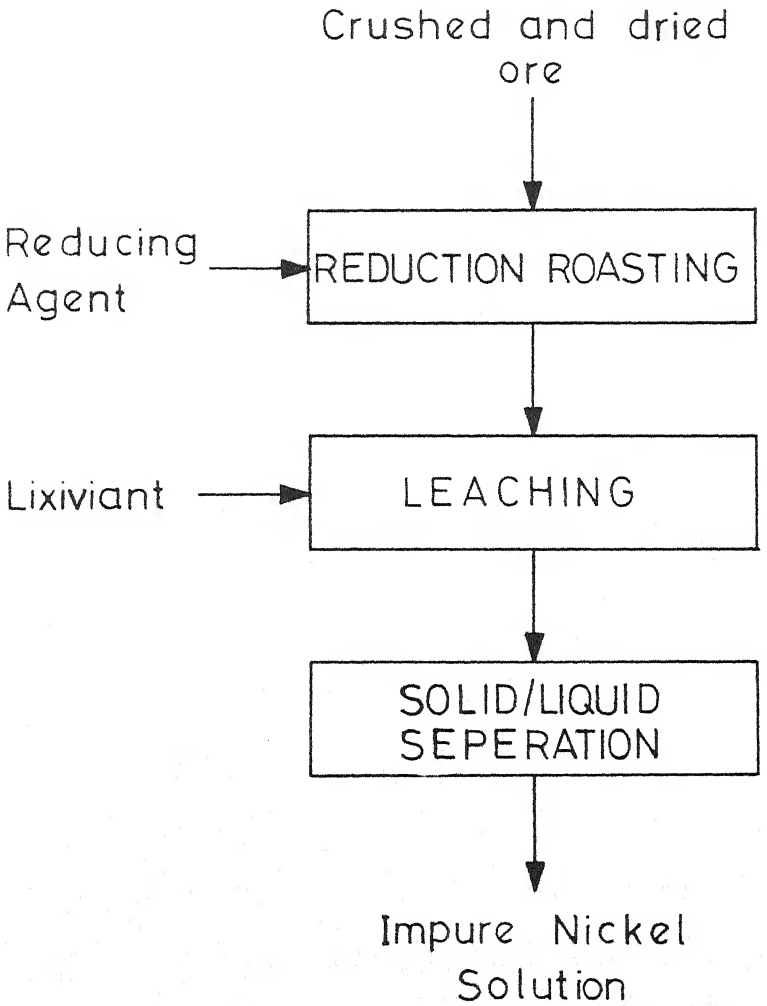

Fig. 2.1. A simplified flowsheet for reduction roast-leaching process.

Reduced nickeliferous laterites have also been reported[38] to be concentrated by magnetic separation technique. The magnetic fraction is leached in ammoniacal ammonium carbonate solution. These are patented processes and additional information is not available. Apostolidis and Distin[19] reduced serpentine ore between 500-900°C by hydrogen and extracted nickel by leaching with aerated H_2SO_4. Reduced laterites[30] and garnierites[31] have also been leached by aerated dilute H_2SO_4 and reported to have given good results. Barbery et al.[21] reduced the oxide ore by a mixture of CO, CO_2 and SO_2 between 650-800°C in presence of 2 percent sodium chloride additive and leached the calcine by dil. H_2SO_4 in an oxidising atmosphere. The reducing gas mixture sulphidised the contents. Sherritt Gordon[32,33] also used a mixture of SO_2 with air for passing through an aqueous slurry of reduced laterite and reported 80-95 percent of nickel and cobalt extraction. This method can be applied to silicate and limonitic ores. Aqueous solutions of sulphur dioxide have also been used for leaching reduced iron ores containing nickel and chromium.[34] Garnierite type of ores were also treated in the same manner after reduction which gave relatively high extraction of nickel[35] but the process has not been commercialised.

Hydrogen has been found to give greater reduction in comparison to that of methane, methane-water, hydrogen-water and CO-CO_2 mixtures.[25,36,37] Caron observed that Hydrogen-Wate

mixtures gave the highest extraction of nickel, however. Siemens and coworkers[20,22,23] reduced the ore by pure carbon monoxide gas in the presence of pyrite followed by leaching in ammoniacal ammonium sulphate. Multistage controlled oxidation leaching gave about 90-92 percent extraction of nickel. Reduction temperatures in the range 350-750°C were used which are much lower than those used by Caron.[25] Tavares et al.[24] used high sulphur coal and pyrite, from the tailings of coal washeries, as reductant at 650-750°C followed by leaching in ammoniacal ammonium carbonate solution in presence of oxygen to extract 88 percent nickel.

The aqueous $CuSO_4$ solution as lixiviant for the reduced laterite ore was studied by Caron[25] and found to give slightly better extraction than the ammoniacal ammonium carbonate solutions. The process was not commercially developed because of the problems of recovery of copper. Recently, Distin[26] has demonstrated that the copper can be regenerated through a flotation operation and may find commercial application.

In the present study, Sukinda laterite ore has been characterised by various chemical and physical methods. The effect of such variables as reduction temperature, hydrogen/water ratio in reducing gas, cooling conditions, type of salt and their concentration, on the heat treatment of the ore has been examined. Various characterisation methods have been used to determine the effect of heating and effectiveness of the reduction was determined by leaching the treated ore in ammonium carbonate solutions.

CHAPTER 3

CHARACTERISATION OF NICKELIFEROUS LATERITIC ORE FROM SUKINDA, ORISSA

3.1 Nickel Analysis

The run-of-mine laterite ore was sieved through various sieves of ASTM standard and each size fraction was separately analysed for nickel content by the procedure described in Appendix I. The weight percent and nickel content of various size fractions is given in Table 3.1. One hundred gm of the -60+100 mesh size fraction was also wet sieved. The fractions were air dried and weight of each fraction of the ore was recorded. The nickel content and weight percent of the weight sieved fractions are presented in Table 3.2.

Since 75 percent of the -60+100 mesh fraction passes through 100 mesh sieve on wet sieving it is concluded that the ore is very soft and made up of very fine particles which are agglomerated to larger particles possibly because of high moisture present in the ore. A comparatively coarse fraction, i.e. -60+100 mesh on wet sieving released particles in all fine size fractions out of which over 40 percent is -400 mesh, i.e. particles smaller than 37 microns. Although dry sieve analysis shows a slight decrease in grade of nickel

TABLE 3.1. Dry Sieve Analysis and Nickel Contents of Nickeliferous Laterite Ore.

Sieve fraction	Weight percent	Ni percent
+30	7	1.25
-30+60	14	1.45
-60+100	38	1.35
-100+140	18	1.30
-140+200	11	1.35
-200+325	9	1.25
-325	3	1.10
	Ore Average	1.32

TABLE 3.2. Wet Sieve Analysis and Nickel Contents of Various Fractions of the -60+100 mesh Dry Sieve Fraction of Nickeliferous Laterite Ore.

Sieve fraction	Weight percent	Ni percent
+100	25.00	1.43
-100+150	12.16	1.30
-150+200	7.94	1.30
-200+300	10.18	1.20
-300+400	3.98	1.25
-400	40.76	1.30
	Ore Average	1.32

in -325 mesh size fraction, wet analysis of the ore shows that its nickel content is about the same as the ore. Scanning Electron Microscopic analysis of the ore shows that the nickel is very finely distributed in iron mineral. The latter has very fine crystallite size. It, therefore, appears that physical separation methods may not be effective for concentration of nickel from this ore, a conclusion reached by several different investigators working with similar ores.

3.2 Surface Area and Pore Size Distribution

The surface area of the ore was determined by the BET method and the specific surface area was found to be 132 m^2/g for the untreated ore. The measurements were done in the laboratories of Bharat Electronics Laboratory, Bangalore. The high surface area of the ore indicates that the ore is highly porous which conforms with other observations reported in this chapter.

The pore size distribution of the ore was determined by mercury porosimeter in the laboratories of the Department of Materials Science and Mineral Engineering at the University of California, Berkeley, California. The results are given in Figure 3.1 for two different size fractions of the ore. Except for the differences in the inter-particle porosity, the pore size distribution is similar for the two size

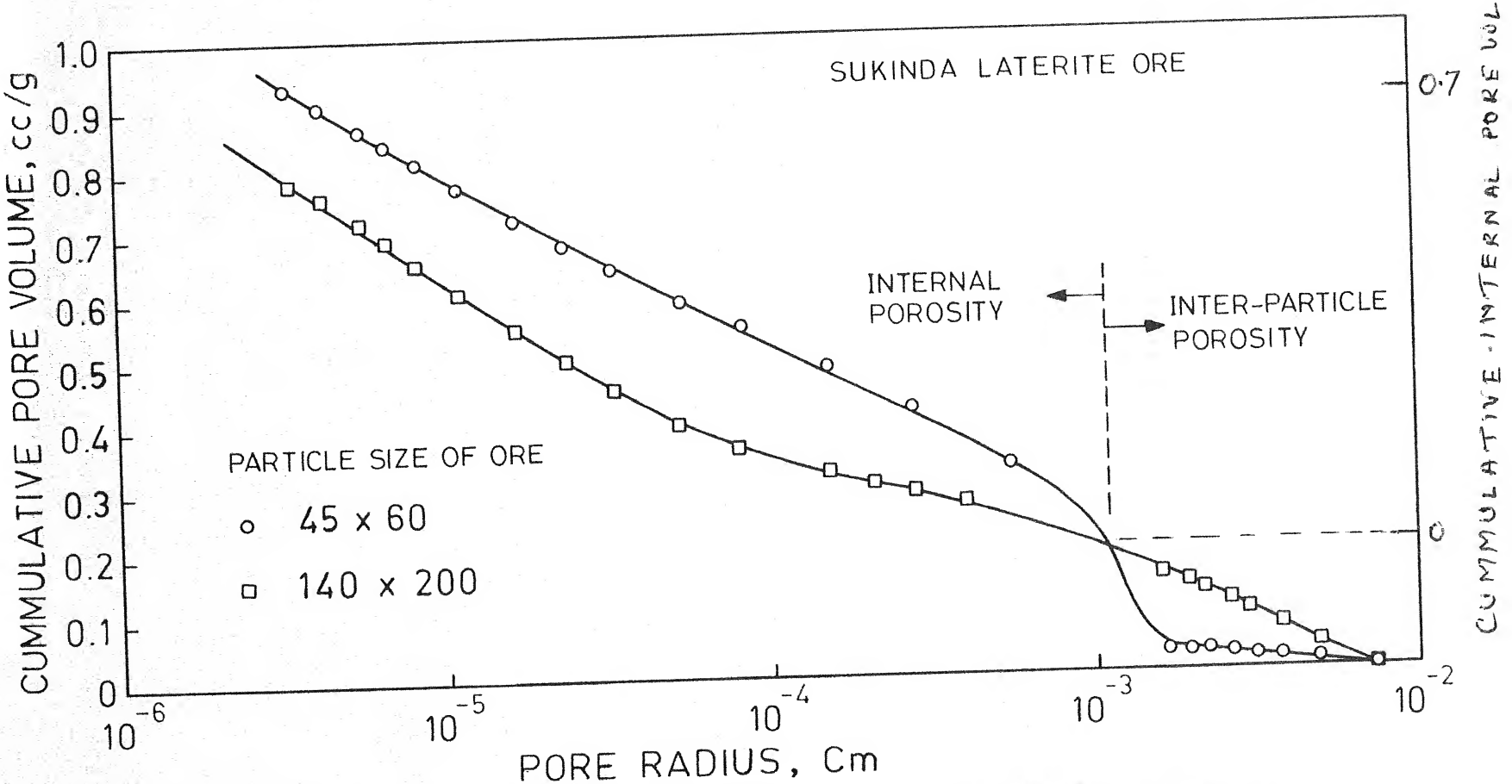

Fig. 3.1. Pore size distribution as determined by mercury porosimeter.

fractions. The 'internal porosity' arises from the packing of very fine particles of the ore which have been observed by the transmission and scanning electron microscopes.

3.3 X-Ray Diffraction

The ore was analysed by X-ray Diffraction unit manufactured by General Electric, U.S.A. with iron target and nickel filter. The X-ray data are presented in Table 3.3. Based on the data the ore predominantly is α-FeOOH. Since the chemical analysis of the ore indicates the presence of many other constituents particularly the SiO_2 in appreciable amount which are not seen in X-ray diffraction patterns it seems that the ore contains amorphous material in gel form. ESCA studies discussed in a subsequent section indicate the presence of Fe(II) in the ore.

3.4 Electron Microscopic Analysis

The laterite ore samples were studied by both Scanning and Transmission Electron Microscopes.* The electron diffraction patterns of the samples were recorded where possible to identify the constituents. Representative scanning micrographs of the ore are presented in Figures 3.2a to 3.2e which show that the ore consists of needle shaped goethite

---

*The SEM studies were carried out at CDRI, Lucknow and at the University of California, Berkeley, and the TEM studies were carried out at IIT Kanpur.

TABLE 3.3. X-ray Diffraction Data for Sukinda Nickel Ore.

d, Å	$(2\theta_{Fe})^{\circ}$	hkl	I/I_1	Component
4.98	22.40	002	0.148	α-FeOOH
4.19	26.70	011	1.000	"
3.39	33.15	-	0.141	"
2.70	41.95	013	0.498	"
2.58	43.95	102	0.262	"
2.45	46.50	111	0.778	"
2.26	50.80	112,103	0.218	"
2.20	52.20	113	0.250	"
1.72	68.35	112	0.323	"
1.56	76.65	115	0.214	"
1.55	79.90	115	0.175	"
1.50	80.10	200	0.175	"
1.45	83.50	202	0.177	"

particles, many of which are agglomerated into larger particles. Although needles of varying sizes are present in the ore, it is seen that needles in a given agglomerate are generally of the same size.

Particles which appear to have rounded shape at lower magnification, say 1000-5000, have been observed to be made of needle shaped particles of much smaller size as seen in Figures 3.2a and 3.2b.

The needle shaped particle marked by the arrow in Figure 3.2a has been shown at higher magnifications in Figure 3.2c and 3.2d. The needle shaped particles appear to have inner structure visible only at higher magnifications. It is not possible to resolve the inner structure at present, but it may be stated that this internal structure gives rise to high surface area and possible complex chemical behaviour of the ore. The needle shaped particles, which have been identified as goethite are clearly visible in the micrograph given in Figure 3.2e.

A transmission micrograph of the ore showing primarily the needle shaped particles or their agglomerates is given in Figure 3.3a. The region marked by circle 1 is shown at a higher magnification in Figure 3.3b with the corresponding diffraction pattern in Figure 3.3c. The electron diffraction data of the circled region in Figure 3.3b is tabulated in Table 3.4. The needle is identified as that of α-FeOOH. The

micrograph in Figure 3.3b also shows that the needle itself has internal fibrous structure. The region marked by circle 2 shows a rod type particle which is shown at a magnification of 22000 in Figure 3.3d. The rod shaped particle appears to be a hollow cylinder which is filled with smaller particles. The needle shaped particle adjacent to the rod again shows fibrous internal structure. Additional micrographs along with the respective electron diffraction patterns are given in Figures 3.4 a to d. The diffraction data for the two samples are tabulated in Tables 3.5 and 3.6.

The data show that the ore is primarily α-FeOOH with small amounts of γ-FeOOH (Lepidocrocite). Figure 3.4c shows that the needle shaped particles are aligned. The alignment comes possibly from the magnetic nature of the needles.

3.5 Thermal Analysis Studies

The differential thermal analysis (DTA) of the Sukinda Nickel ore was done in the laboratories of the Department of Chemical Engineering, Monash University, Victoria, Australia and results of the same are presented as curve 1 in Figure 3.5 along with the DTA results of some other nickeliferous lateritic ores. Curves 1 to 5 are for limonitic ores, curve 6 is for a mixed ore and curves 7 to 10 are for silicate ores. The endothermic peak in the temperature range 300-400^{o}C is for the transformation of goethite to hematite.

Fig. 3.2a: SEM Micrograph of Sukinda laterite ore, X 1000, showing rounded and rod shaped particles.

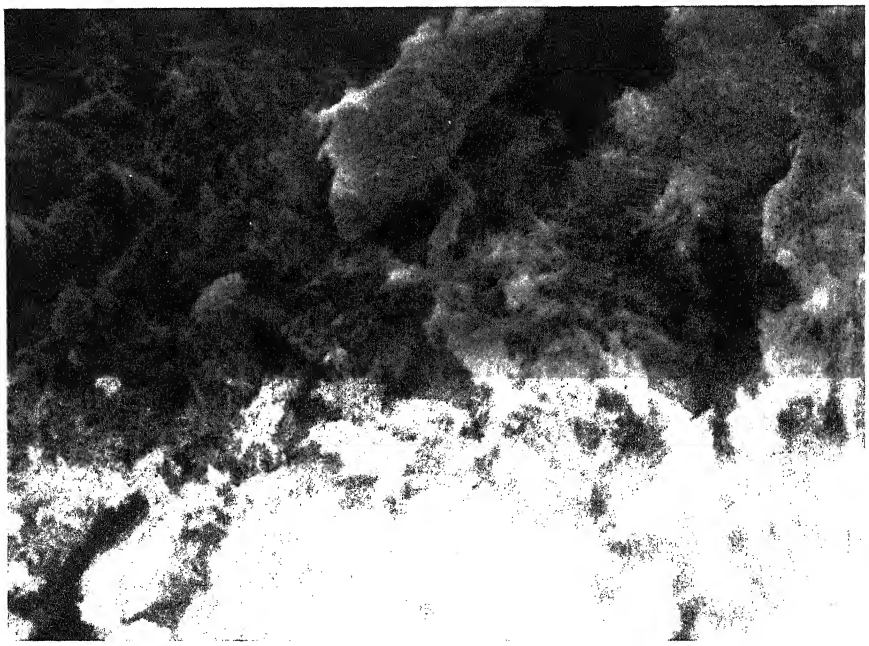

Fig. 3.2b: SEM Micrograph Sukinda laterite ore X 20000 showing needle shaped structure of Goethite.

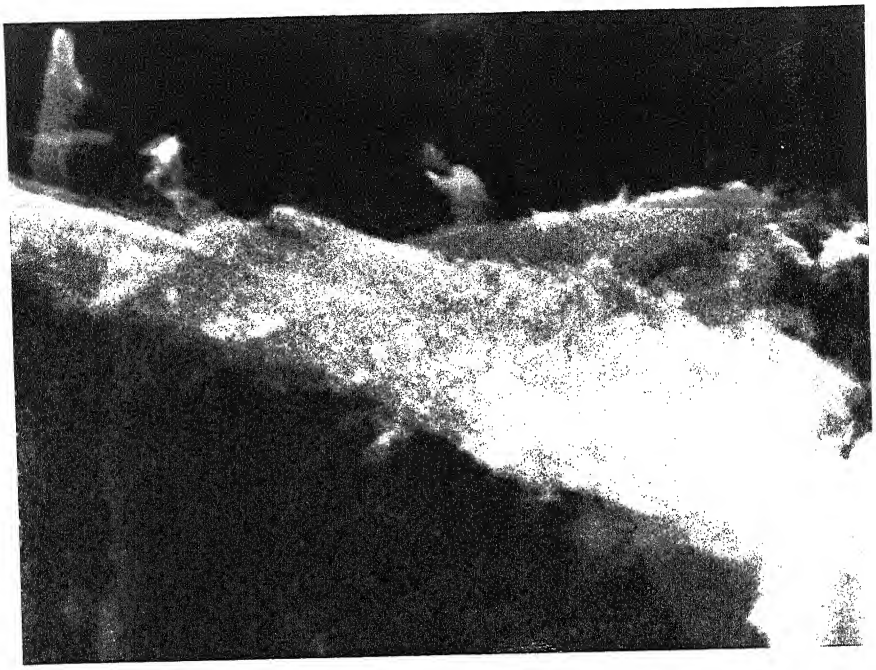

Fig. 3.2c: SEM Micrograph of Sukinda laterite ore X20000 showing highly porous and internal structure.

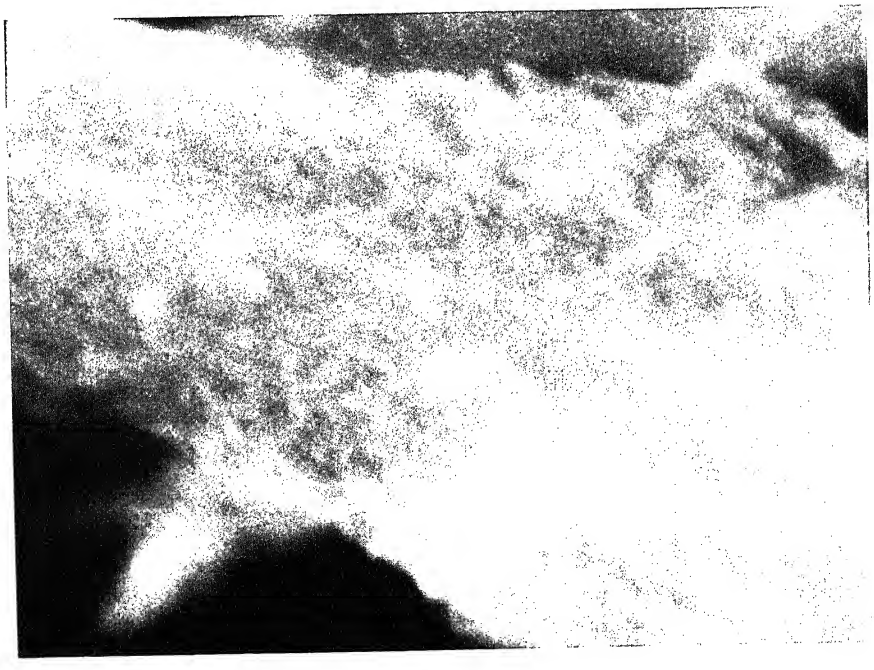

Fig. 3.2d: SEM Micrograph of Sukinda laterite ore X50000 showing highly porous surface and internal structure.

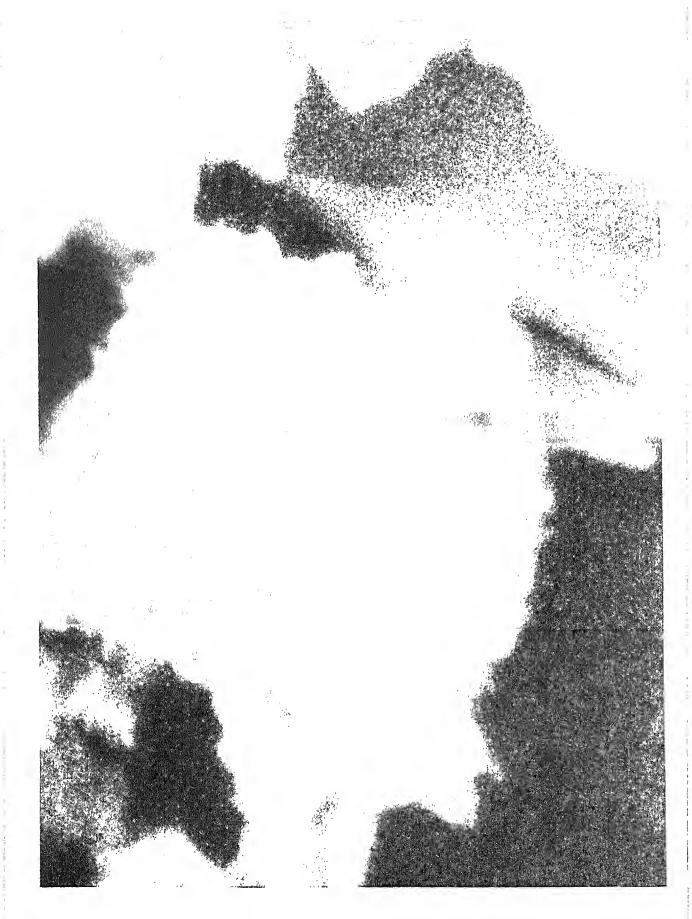

Fig. 3.2e: SEM Micrograph of Sukinda laterite ore, X20000 showing needle shaped particles in the ore.

(a)

(b)

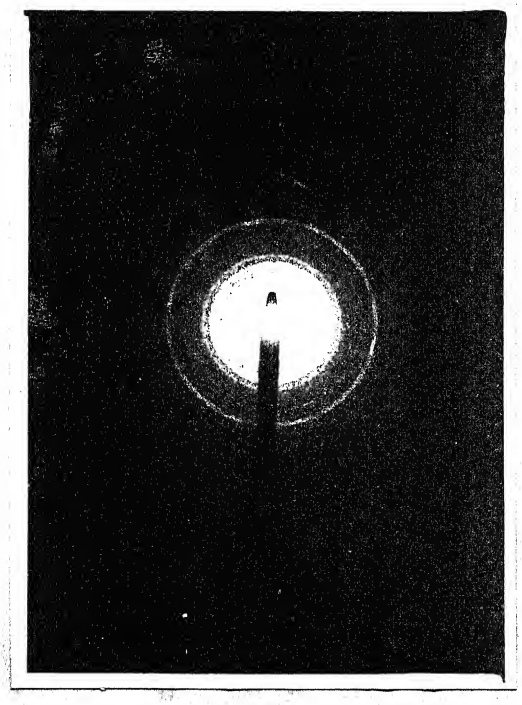

(c)

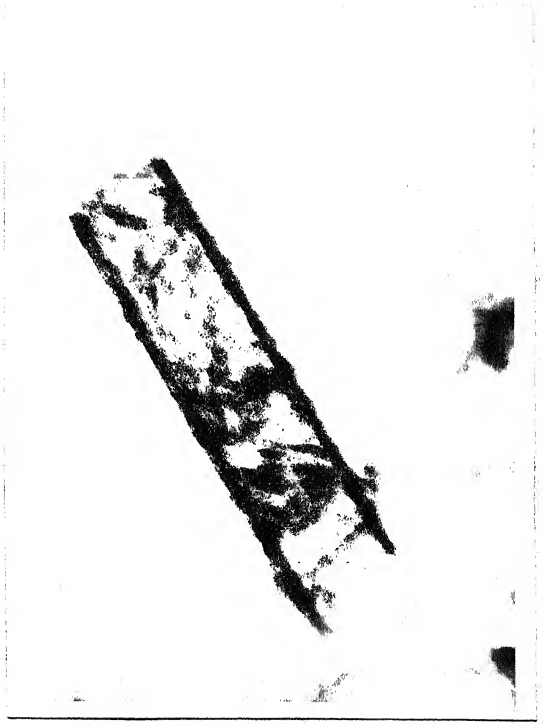

(d)

Fig. 3.3. TEM Micrograph of Sukinda laterite ore showing
(a) needle and rod shaped particles and agglomerates, X1700,
(b) particle marked 1 in Fig. 3.3(a), X22000,
(c) Electron Diffraction Pattern for particle in 3.3(b), and
(d) Particle marked 2 in 3.3(a), X22000 showing rectangular rod with internal hollow structure.

(a)

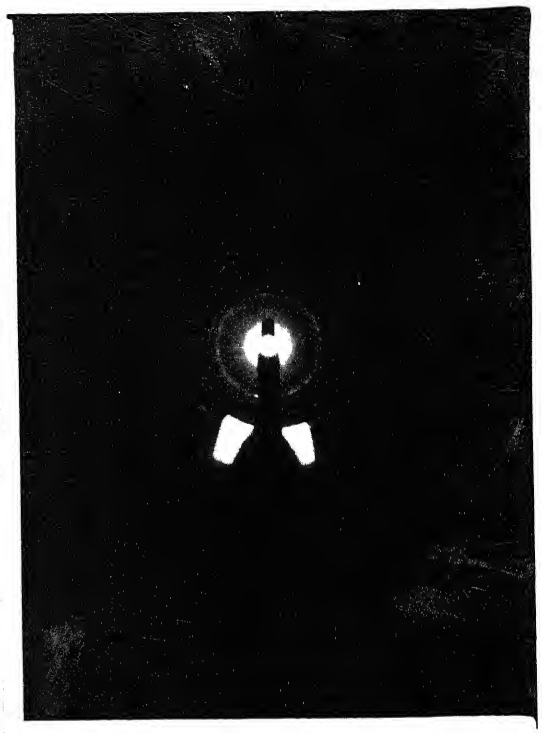

(b)

(c)

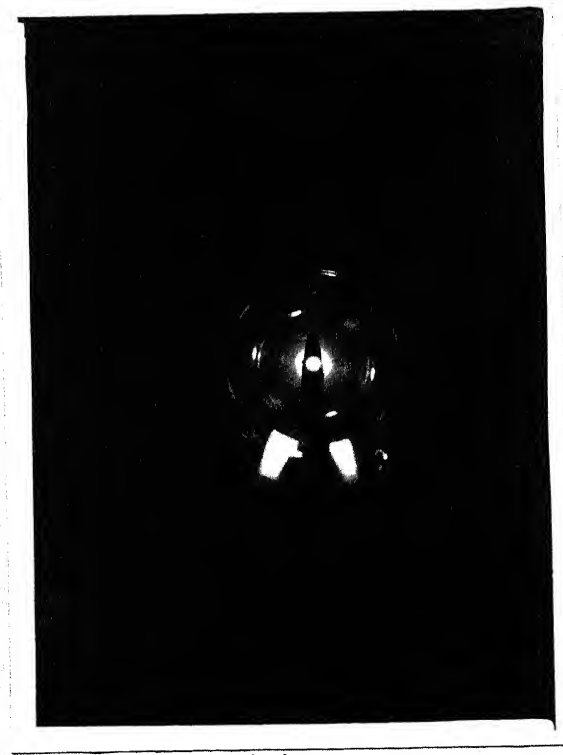

(d)

Fig. 3.4. TEM Micrograph of Sukinda laterite ore showing.
(a) Needles, X10000,
(b) Electron Diffraction Pattern for the particle marked in Fig. 3.4(a),
(c) Needle structure in criss-cross formation, and
(d) Electron Diffraction Pattern for the particle marked in Fig. 3.4(c).

TABLE 3.4. Electron Diffraction Data for Sukinda Nickel Ore Particle in Figure 3.3c (-65+100 Mesh Size).

R_i in cm	Relative Intensity	d, Å	Line Identification*
1.25	S	2.719	α-FeOOH
1.50	VS	2.267	"
1.80	W	1.888	"
2.17	VW	1.566	"
2.34	VW	1.453	"
2.55	MS	1.333	"

TABLE 3.5. Electron Diffraction Data for Sukinda Nickel Ore Particle in Figure 3.4b (-325 Mesh Size).

R_i in cm	Relative Intensity	d, Å	Line Identification*
0.96	MS	3.540	α-FeOOH
1.30	W	2.615	"
1.38	VS	2.463	"
1.60	MW	2.124	"
1.93	VW	1.761	"
2.10	VW	1.619	"
2.44	S	1.393	"

*Identified by comparison with standard ASTM diffraction data.

TABLE 3.6. Electron Diffraction Data for Sukinda Nickel Ore Particle in Figure 3.4d (-325 Mesh Size).

R_i in cm	Relative Intensity	d, Å	Line Identification*
0.460	VW	3.694	-
0.435	VW	3.907	-
0.775	VS	2.193	α-FeOOH
0.680	S	2.499	"
0.875	VS	1.942	"
1.000	W	1.699	"
1.240	MS	1.371	"
1.250	MS	1.359	"
1.300	VS	1.307	"
1.400	VW	1.214	γ-FeOOH
1.400	VW	1.214	"
1.500	VW	1.133	"

*Identified by comparison with standard ASTM diffraction data.

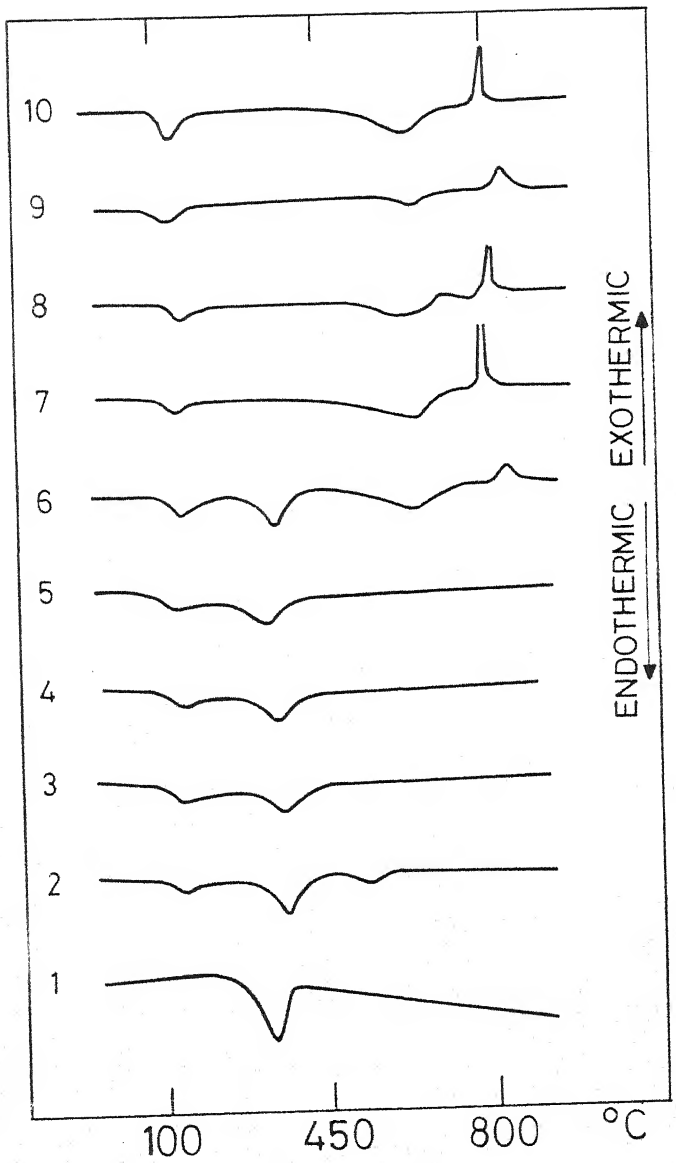

Fig. 3.5. Differential thermal curves of nickel ores.
Curve 1: Sukinda laterite ore
Curve 2-10: Reference 15.

$$2\alpha\text{-FeOOH} \longrightarrow \alpha\text{-}Fe_2O_3 + H_2O.$$

The exact value of the transformation temperature depends upon the crystallite size and the nature and amount of isomorphically substituted impurities in the solid. From surface energy considerations it is expected that the transformation temperature will decrease with reduction in crystallite size. Kulp and Trites[39] found that, in general, hydrous ferric oxides gave a lower peak temperature with decrease in grain size. The area under the DTA curve remained unchanged, however. Well crystallised goethite gives a single endothermic peak at a temperature of 350-390°C[40] whereas poorly crystalline goethite gives peaks at 300°C or at still lower temperatures.[41] Laboratory investigations have shown that the presence of isomorphically substituted aluminium in goethite can lower the goethite to hematite transformation temperature by as much as 50°C.[42]

A compilation of the data for various iron oxide and silicate minerals is given in Table 3.7.[44] On the basis of the DTA data it is possible to classify the nickeliferous lateritic ore into three types.

1. Limonitic or oxide type ores
2. Serpentinic or silicate type ores
3. Mixed ores (ores containing both limonitic and silicate varieties).

The goethite to hematite transformation temperature provides useful qualitative information regarding the crystalline nature of the ore. The presence of very fine crystals of goethite has been confirmed by the electron microscopic studies. A change in the ore size fraction used for the DTA study from 45x60 mesh to 140x200 mesh did not change the transformation temperature. The DTA plots for various iron oxides and hydroxides and their mixtures are presented in Figure 3.6.[43] On a comparision of the DTA plot for Sukinda Laterite ore with these plots it can be concluded that the ore contains poorly crystallised goethite.

The thermal gravimetric analysis (TGA) study gave a loss of 8.57 percent in weight for the goethite to hematite transformation. Pure goethite is expected to show a weight loss of 10.11 percent. Smaller weight loss than the expected value for pure goethite shows that the ore contains some other minerals. If it can be assumed that the weight loss at 312°C is only due to goethite to hematite transformation, the ore is estimated to contain 84.84 percent goethite.

3.6 ESCA Studies

The Electron Spectroscopy for Chemical Analysis (ESCA) studies were conducted on the Sukinda laterite ore in the laboratories of the University of California, Berkeley, U.S.A. The spectra is presented in Figure 3.7 and the corresponding data are tabulated in Table 3.8. The table lists the binding

TABLE 3.7. Differential Thermal Analysis Data of Iron Oxide and Silica.[44]

Nature of transformation	Formula	Endothermic Reaction, °C	Exothermic Reaction, °C
Goethite → Hematite	α-FeOOH	411	
Limonite → Hematite	α-FeOOH	340	423 475
Lepidocrocite → Hematite	γ-FeOOH	345	470
Curie Point (Hematite)	α-Fe_2O_3	675	
Curie Point (Magnetite)	Fe_3O_4	450-590	300-450 480-700
Inversion Quartz	SiO_2	520-578	
Allophane	$SiO_2 \cdot 2Al_2O_3$	112	960

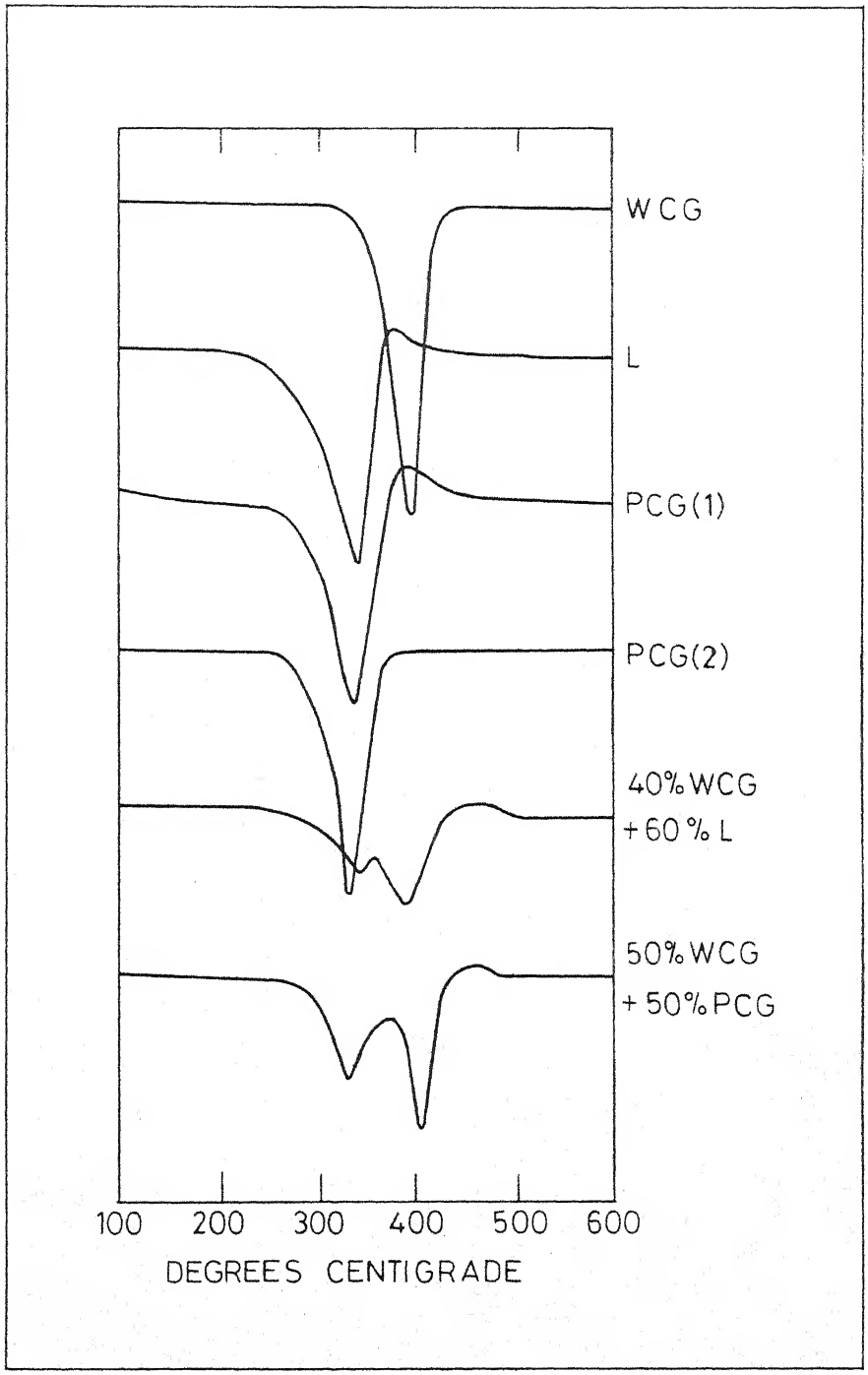

Fig. 3.6. DTA curves for various iron oxides and hydroxides.[43]
WCG: Well Crystallized Goethite,
L : Lepidocrocite
PCG: Poorly crystallized Goethite.

TABLE 3.8. The Area under the ESCA Peaks for Sukinda Nickel Ore.

Peak	Binding energy, eV	Area (arbitrary units)	Area Ratio Basis Fe(II)
Fe(II)	709.80	23.94	1.000
Fe(III)	712.10	23.52	0.983

energies for $2P_3$ electrons in the iron oxide of the ore for Fe(II) and Fe(III) oxidation states respectively. The binding energies for $2P_3$ electrons in Fe metal, Fe(II) and Fe(III) for various compounds are presented in Table 3.9. Although there is some scatter in the values for binding energies reported in the literature, the binding energy increases in the order Fe < Fe(II) < Fe(III).

The relative amounts of Fe(II) and Fe(III) are given by the area under the peaks. The area ratio of 0.983 for area of Fe(III)/area of Fe(II) means that in the Sukinda Laterite ore Fe(II) and Fe(III) are almost equal in amount. On the basis of the X-ray diffraction, Electron Microscopic and DTA studies the iron oxide present in the ore is predominantly goethite. There was no indication of the presence of iron in Fe(II) state. The ESCA studies, on the other hand, report almost equal amount of iron in Fe(II) and Fe(III) forms. The discrepancy between ESCA studies and the other studies

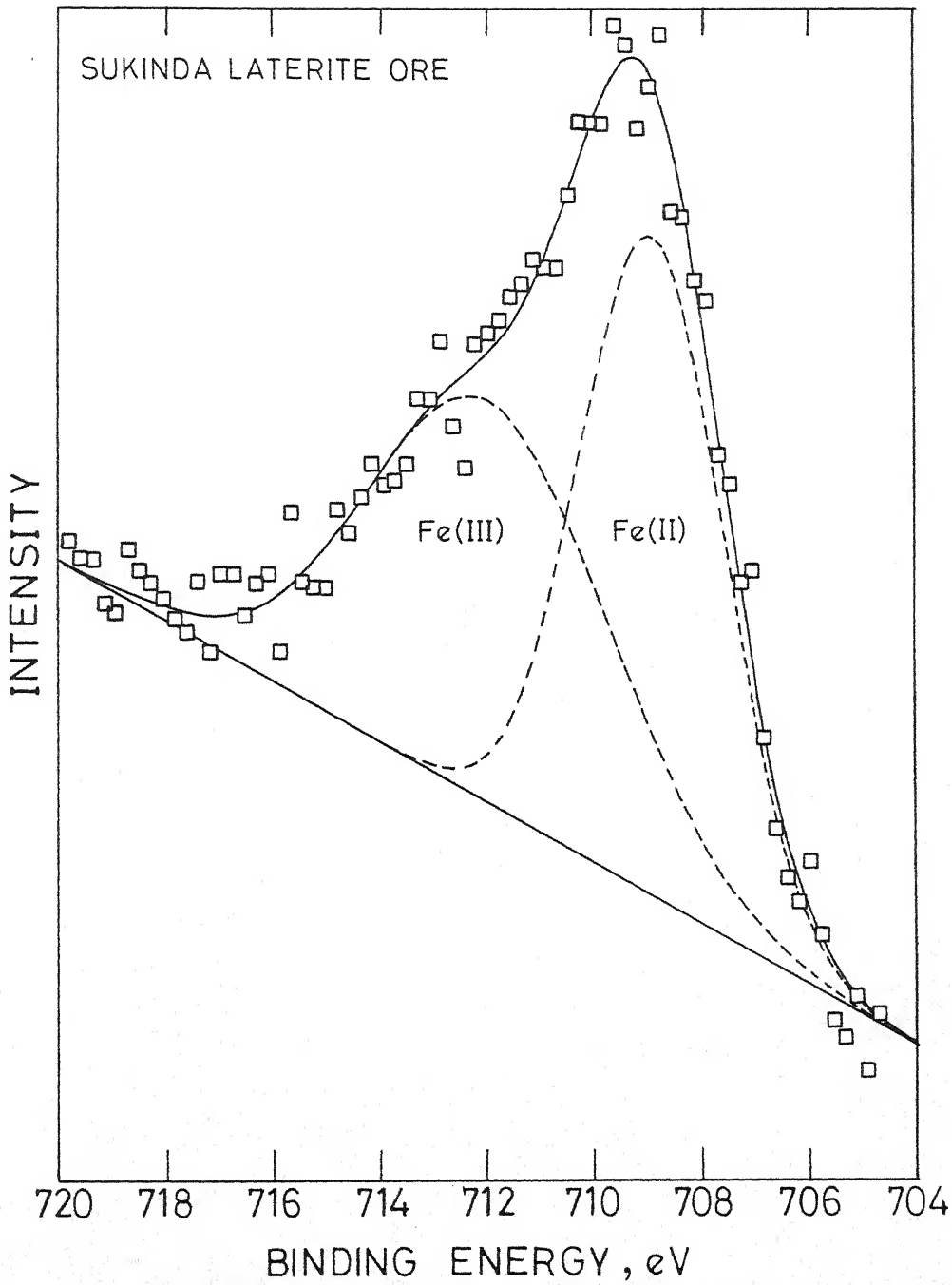

Fig. 3.7: ESCA curves for Fe(II) and Fe(III) in the ore.

may be explained on the basis that in ESCA primarily the surface of the ore is analysed whereas the other techniques reported herein give analysis of the bulk of the sample. Thus, it seems that Fe(II) is present primarily in the surface layer of the mineral particles. In addition, the failure to observe Fe(II) in the X-ray diffraction and electron microscopy studies may be due to the fact that Fe(II) is present as amorphous material.

TABLE 3.9. The ESCA Binding Energies for Iron in Various Compounds and Minerals.

Compounds and Minerals	B.E. Fe, eV	B.E. Fe(II), eV	B.E. Fe(III), eV	Ref.
Fe metal	707.3			46
	706.9			47
	708.2			48
	706.2			49
FeO		710.3		46
		707.9		47
		708.6		50
FeF_2		711.5*		45
$FeCl_2$		710.8		45
$FeBr_2$		710.5		45
FeS		710.5		45
$K_4Fe(CN)_6$		708.7		45
$Zn_2Fe(CN)_6$		708.2		45
Fe_2O_3			711.5	45
			711.4	46
			711.1	47
			712.4	48
			711.5	49
			711.8	50
FeF_3			714.4*	45
$FeCl_3$			711.5	45
$FeBr_3$			710.3	45
K_3FeF_6			714.6*	45
Fe_3O_4			711.4	46
			710.4	47
			709.0	49
α-FeOOH			711.0	45
Sukinda Ni Ore		709.80	712.10	Present work

*The values are high because of higher electronegativity of fluorine.

CHAPTER 4

PRETREATMENT OF THE ORE FOR LEACHING

4.1 Introduction

In the reduction roast/leaching process for extraction of nickel from the laterite ore reduction is a very critical step as discussed in Chapter 2. To make the nickel in the ore soluble in ammoniacal solutions, it is necessary to chemically alter the ore. The effect of a number of operating variables on heat treatment of the Sukinda Laterite ore has been studied. The variables investigated include the reducing environments, reduction temperature etc.

4.2 Procedure

A 2 gm sample was heated in a tube furnace as shown in Figure 4.1 in the desired atmosphere of Argon, Hydrogen or Hydrogen-Water mixture for 3 hours. The temperatures used were mainly 200°, 400°, 600°, 700° and 800°C. After the desired temperature was attained the reaction tube was flushed with purified Nitrogen for 10 minutes and the ore sample in an alundum or stainless steel boat was introduced from the gas exit end of the furnace. A flow of purified reducing gas at a rate of 110 bubbles per minute was maintained

through out the reduction period which lasted for about 3 hours. At the end of the reduction period the cooling gas, N_2 or Ar was passed through the furnace for 10 minutes and then the sample was allowed to cool at the gas exit end of the furnace for preset period.

The H_2-H_2O mixtures for reduction were prepared by passing H_2 gas through a humidifier in which purified hydrogen gas flow through a series of bubblers half-filled with distilled water submerged fully in a water bath maintained at a temperature of 85°C as shown schematically in Figure 4.1. To prevent condensation of water vapour the connecting glass tubes were heated by passing current through a resistence wire wound around the tube which was insulated with asbestos tape. The bath temperature of 85°C gave a hydrogen/water ratio of 60/40. The ratio was determined by absorbing the H_2O vapor in a preweighed tube filled with calcium chloride and silica gel. The weight of the water was determined by weighing the tubes after a certain amount of hydrogen had passed through the tube. A Weight Test Meter attached to the end tube gave the volume flow of hydrogen. The H_2/H_2O ratio was checked at 200°, 400°, 600° and 800° and was observed to be independent of the furnace temperature.

The heat treated samples were characterised as discussed in the following sections.

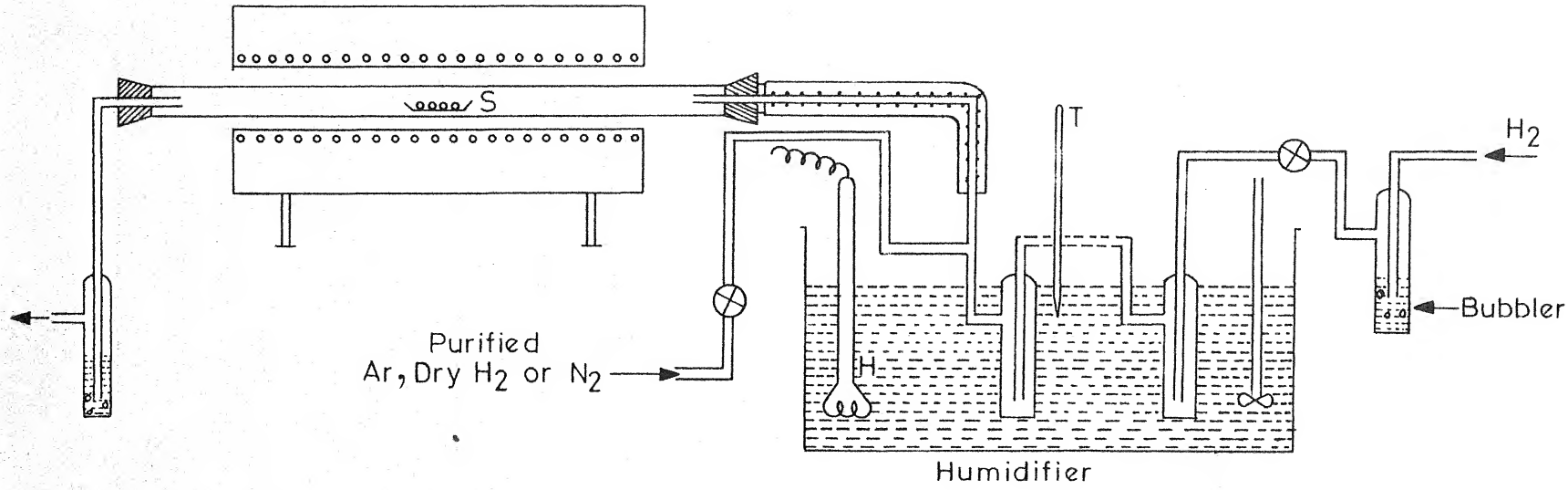

Fig. 4.1: Schematic diagram of humidifier and heat treatment apparatus.

T: Thermometer
H: Heater
S: Sample Boat.

4.3 Pretreatment in Argon

The surface area of the ore heat treated in Argon atmosphere at different temperatures for 3 hours is given in Table 4.1. These measurements were done by BET method in the laboratories of Bharat Electronics Limited, Bangalore. The specific surface area gradually decreases with increase in temperature indicating sintering. On the basis of ESCA and other studies it has been postulated that the ore contains, at least on the surface, an amorphous or gel type of solid containing ferrous ions. It is likely that this material undergoes transformations during heating leading to sintering or agglomeration of the particles. Joining of the particles by the formation of a new phase is likely to reduce the effective surface area.

TABLE 4.1. Surface Area of Sukinda Laterite Ore after Heat Treatment in Argon for 3 Hours.

Treatment Temperature, ^{o}C	Specific Surface Area, m^2/g
Untreated	132
200	116
400	84
600	47
800	30

The X-ray diffraction data of the Argon heat treated samples at various temperatures are given in Table 4.2. For comparison the data for untreated ore has also been tabulated. On heating to 200°C goethite in the ore remains unchanged. No new phase was observed at this temperature. At higher temperatures, i.e. 400°C and 600°C the goethite transforms completely to α-Fe_2O_3. The DTA experiments discussed in Chapter 3 show that the goethite decomposes at a temperature of 312°C. At 800°C a small amount of magnetite also forms because of the slightly reducing power of the argon gas. The X-ray peaks become sharper at 600°C than at 400°C indicating growth of crystallite size which is confirmed by decrease in surface area of the ore.

Electron Diffraction studies of the samples were carried out in Transmission Electron Microscope. It seems that the sample dispersed in water medium reacted with water and as a result the sample constituents got transformed. Electron diffraction studies were therefore not pursued.

4.4 Pretreatment in Dry Hydrogen

The X-ray diffraction data for the samples heat treated in dry hydrogen at 200°, 400° and 600°C are given in Table 4.3. At 200°C the constituents present are small amount of α-FeOOH, Fe_3O_4 and α-Fe_2O_3. At 400°C, the products of reaction are α-Fe and Fe_3O_4. The amount of Fe_3O_4 is significantly larger

TABLE 4.2: X-ray Diffraction Data for Sukinda Laterite Ore Heat Treated in Argon for 3 hrs.

S.No.	d, Å	hkl	Untreated		200°C		400°C		600°C		800°C	
			I/I_{max}	Component	I/I_{max}	Component	I/I_{max}	Component	I/I_{max}	Component	I/I_{max}	Component
1	2	3	4	5	6	7	8	9	10	11	12	13
1	4.98	002	0.148	α-FeOOH	-	-	-	-	-	-	-	-
2	4.19	011	1.0	α-FeOOH	0.587	α-FeOOH	-	-	-	-	-	-
3	3.66-3.69	-	-	-	-	-	0.233	$\alpha-Fe_2O_3$	0.248	$\alpha-Fe_2O_3$	0.270	$\alpha-Fe_2O_3$
4	3.39	-	0.141	α-FeOOH	-	-	-	-	-	-	-	-
5	2.96-2.91	-	-	-	-	-	-	-	-	-	0.125	Fe_3O_4
6	2.69	013	0.498	α-FeOOH	0.952	α-FeOOH	0.80	$\alpha-Fe_2O_3$	0.948	$\alpha-Fe_2O_3$	1.000	$\alpha-Fe_2O_3$
7	2.58	102	0.262	α-FeOOH	-	-	-	-	-	-	-	-
8	2.51	-	-	-	-	-	-	-	-	-	-	-
9	2.45	111	0.778	α-FeOOH	1.0	α-FeOOH	1.0	$\alpha-Fe_2O_3$	1.0	$\alpha-Fe_2O_3$	0.895	$\alpha-Fe_2O_3$ + Fe_3O_4
10	2.43	-	-	-	-	-	-	-	-	-	-	-
11	2.26	112, 103	0.218	α-FeOOH	0.619	α-FeOOH	-	-	-	-	-	-
12	2.20	113	0.250	α-FeOOH	0.317	α-FeOOH	0.316	$\alpha-Fe_2O_3$	0.306	$\alpha-Fe_2O_3$	0.250	$\alpha-Fe_2O_3$

...Contd.

Table 4.2 (Contd.)

1	2	3	4	5	6	7	8	9	10	11	12	13
13	2.19	-	-	-	0.428	α-FeOOH	-	-	-	-	-	-
14	1.83	024	-	-	-	-	0.241	α-Fe_2O_3	0.318	α-Fe_2O_3	0.322	α-Fe_2O_3
15	1.72	113	0.323	α-FeOOH	0.634	α-FeOOH	-	-	-	-	-	-
16	1.69	116	-	-	-	-	0.50	α-Fe_2O_3	0.525	α-Fe_2O_3	0.447	α-Fe_2O_3
17	1.56	115	0.214	α-FeOOH	-	-	-	-	-	-	-	-
18	1.50	200	0.175	α-FeOOH	-	-	-	-	-	-	-	-
19	1.45	202	0.177	α-FeOOH	-	-	-	-	-	-	-	-

at this temperature. At 600°C still higher amount of α-Fe forms. In addition to Fe_3O_4, FeO, α-Fe and Fe-Ni alloy are also formed. These transformations are expected on the basis of the Fe-H-O diagram shown in Figure 4.2. The transformation $Fe_2O_3 \rightarrow Fe_3O_4 \rightarrow FeO \rightarrow Fe$ is possible even with small amount of hydrogen. But kinetics of reduction depends on the temperature. It is evident that reaction kinetics is slow at 400°C. Hence formation of α-Fe is less than that at 600°C. The nickel in the ore due to local higher concentration forms an Fe-Ni alloy rather than metallic nickel as no peak for Ni metal was observed. The formation of an Fe-Ni alloy and α-Fe suggests that there may be some localised concentration as a separate nickel or iron-nickel mineral with remainder of Fe present as nickel free mineral. No evidence for nickel rich mineral could be found in the microscopic investigations up to a magnification of 50,000, however.

4.5 Pretreatment in Hydrogen-Water Mixtures

Effect of Heat Treatment Temperature: The samples heat treated at different temperatures were examined by different techniques. The X-ray diffractograms of heat treated samples are presented in Fig. 4.3 and the related data is given in Table 4.4. At 200°C, the ore remains unaltered as α-FeOOH. At 400° and 600°C the Fe_3O_4 forms which is expected on the basis of the Fe-H-O equilibrium diagram given in Figure 4.2.

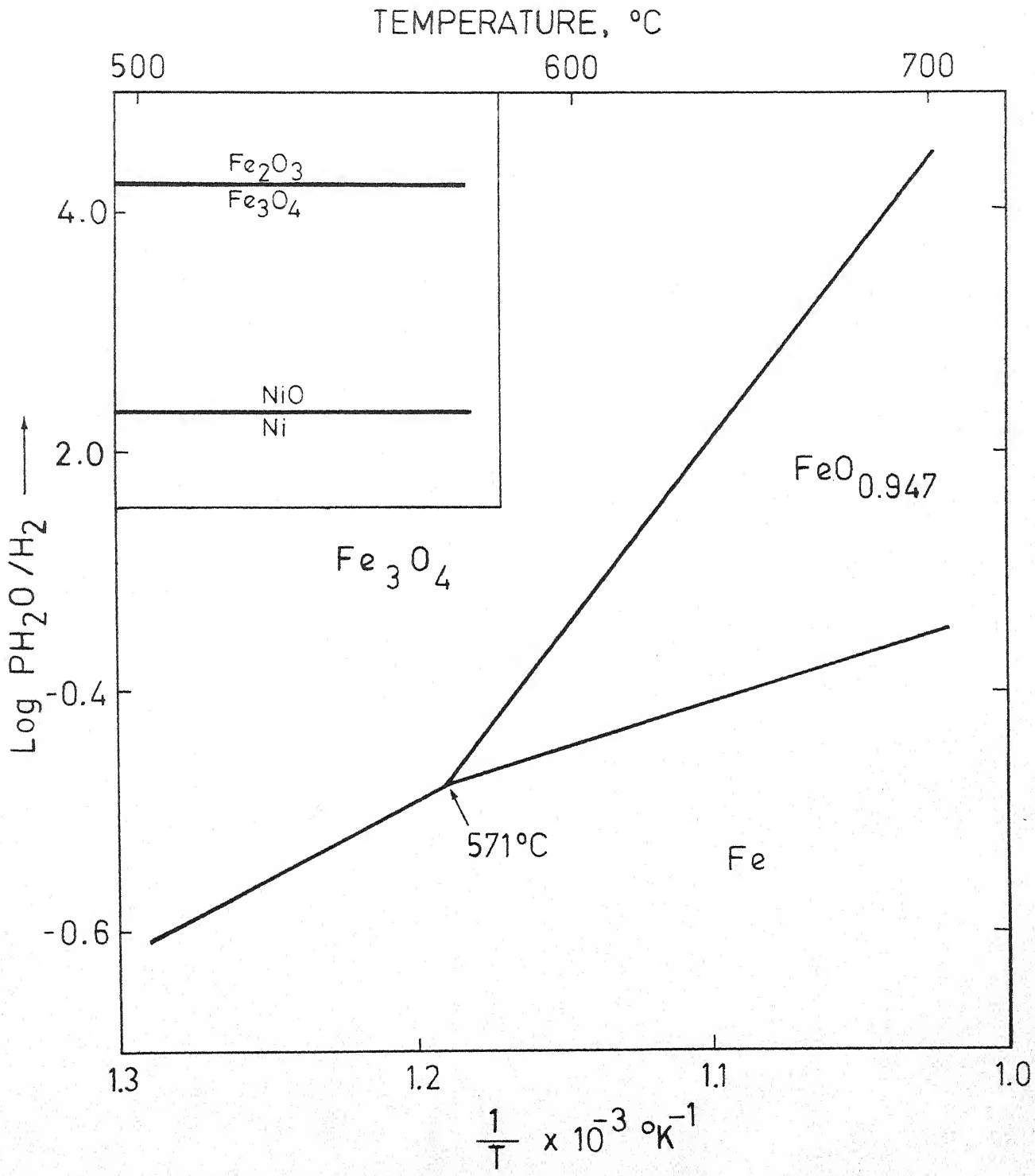

Fig. 4.2. Fe-H-O and Ni-H-O equilibrium diagram.

TABLE 4.3. X-ray Diffraction Data for Sukinda Laterite Ore Heat Treated in Dry Hydrogen for 3 hours

S.No.	d, A^{o}	hkl	Untreated		200°C		400°C		600°C	
			I/I_{max}	Component	I/I_{max}	Component	I/I_{max}	Component	I/I_{max}	Component
1	2	3	4	5	6	7	8	9	10	11
1	4.98	002	0.148	α-FeOOH	-	-	-	-	-	-
2	4.78	111	-	-	-	-	0.20	Fe_3O_4	-	-
3	4.19	011	1.0	α-FeOOH	0.292	α-FeOOH	-	-	-	-
4	-	-	-	-	-	-	-	-	-	-
5	3.39	0.141		α-FeOOH	0.170	$\alpha-Fe_2O_3$	-	-	-	-
6	2.93-2.95	-	-	-	-	-	0.458	Fe_3O_4	0.07	Fe_3O_4
7	2.76	-	-	-	-	-	0.116	Fe_3O_4	-	-
8	2.70	013	0.498	α-FeOOH	0.902	$\alpha-Fe_2O_3$ +α-FeOOH	-	-	-	-
9	2.58	107	0.262	α-FeOOH	-	-	-	-	-	-
10	2.51	110	-	-	1.0	$\alpha-Fe_2O_3$ $+Fe_3O_4$	1.0	Fe_3O_4	0.352	Fe_3O_4
11	2.45	111	0.778	α-FeOOH	0.292	α-FeOOH	-	-	-	-
12	2.26	112, 103	0.218	α-FeOOH	-	-	-	-	-	-

...Contd.

Table 4.3 (Contd.)

1	2	3	4	5	6	7	8	9	10	11
13	2.20	113	0.250	α-FeOOH	0.414	α-Fe_2O_3	-	-	0.250	FeO
14	2.06-2.09	-	-	-	-	-	0.50	Fe_3O_4	0.275	Fe-Ni
15	2.024	110	-	-	-	-	0.35	α-Fe	1.0	α-Fe
16	1.78	-	-	-	-	-	-	-	0.095	Fe-Ni
17	1.70	116	0.323	α-FeOOH	-	-	0.15	Fe_3O_4	-	-
18	1.60	018	-	-	-	-	0.45	Fe_3O_4	-	-
19	1.56	115	0.214	α-FeOOH	-	-	-	-	-	-
20	1.50	200	0.175	α-FeOOH	-	-	-	-	-	-
21	1.45	202	0.177	α-FeOOH	-	-	-	-	-	-

Due to low concentration of the reducing gas further reduction is not possible at 600°C. At 700°C, α-Fe, FeO and Fe-Ni alloy are also observed. At 800°C, appreciable quantity of α-Fe is formed but FeO completely disappears. The formation of α-Fe is not expected thermodynamically. Its formation is possibly because of more reducing atmosphere prevailing in the unexposed region of boat containing the sample. The scanning electron micrographs of the sample heat treated at 600° and 800°C are presented in Figure 4.4a-d. At 600°C the particle continues to show highly porous structure with a few needle shaped primary particles as shown in Figure 4.4 a-c. At 800°C the needle shaped particles disappear and irregular particles with rounded corners are formed. The product at 800°C is a mixture of Fe and Fe_3O_4 and consists of agglomerates of fine particles and is still highly porous. ESCA studies carried out in the laboratories of the University of California, Berkeley, U.S.A. indicated higher Fe(II)/Fe(III) ratio for the samples heat treated at 800°C in comparison to that of the 600°C as shown in Table 4.5. DTA plot shown in Figure 4.5 for the sample heat treated at 600° and 700°C indicate relatively lower FeO and higher Fe_3O_4 content in the former and higher FeO and lower Fe_3O_4 content in the latter.

Based on these studies it may be concluded that the iron in the ore gets reduced to metallic Fe in several stages.

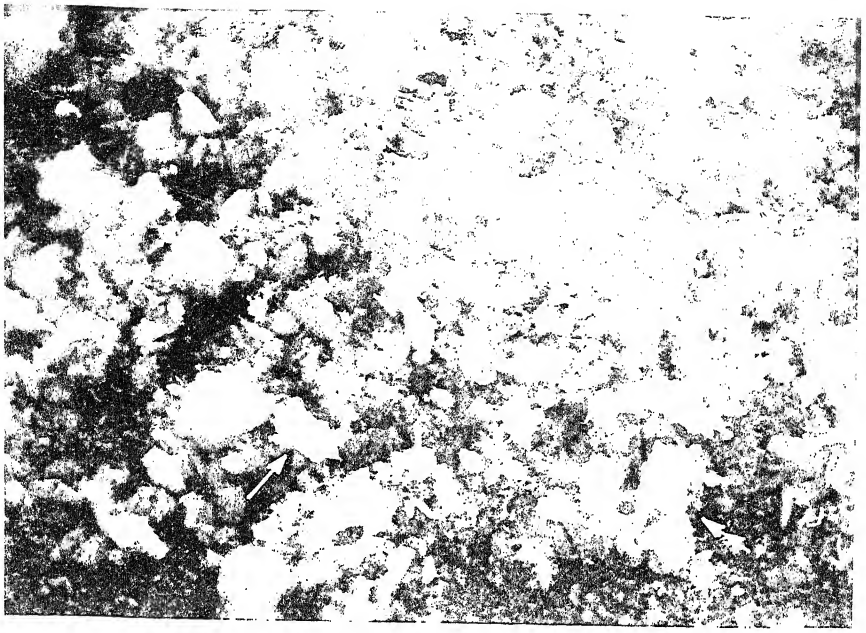

Fig. 4.4(a). SEM micrograph of the sample heat treated at 600°C, X1000, showing the shape of the particles.

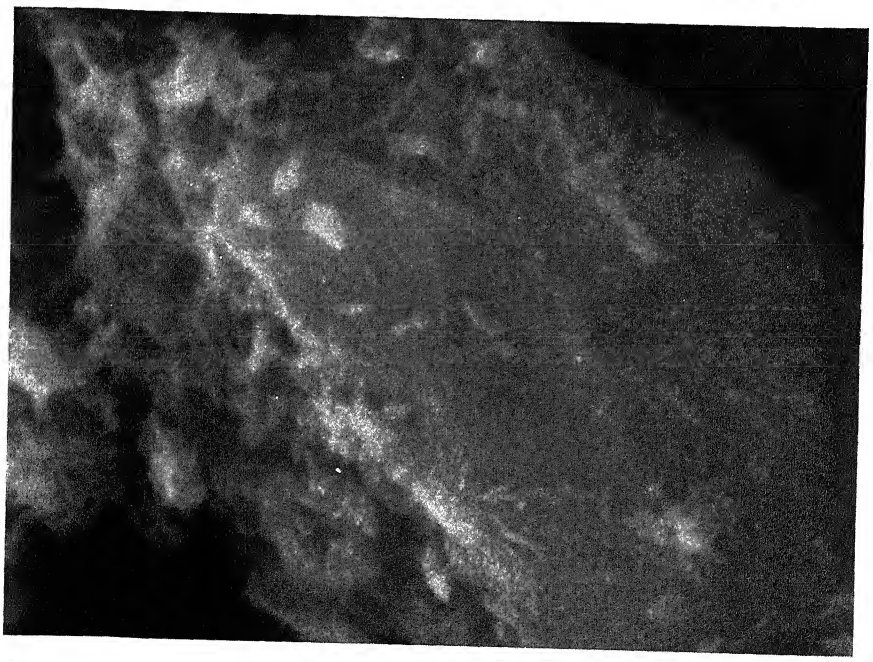

Fig. 4.4(b). SEM micrograph of the single arrow marked, particle in Fig. 4.4(a), X20000 showing needle shaped particles and highly porous surface structure.

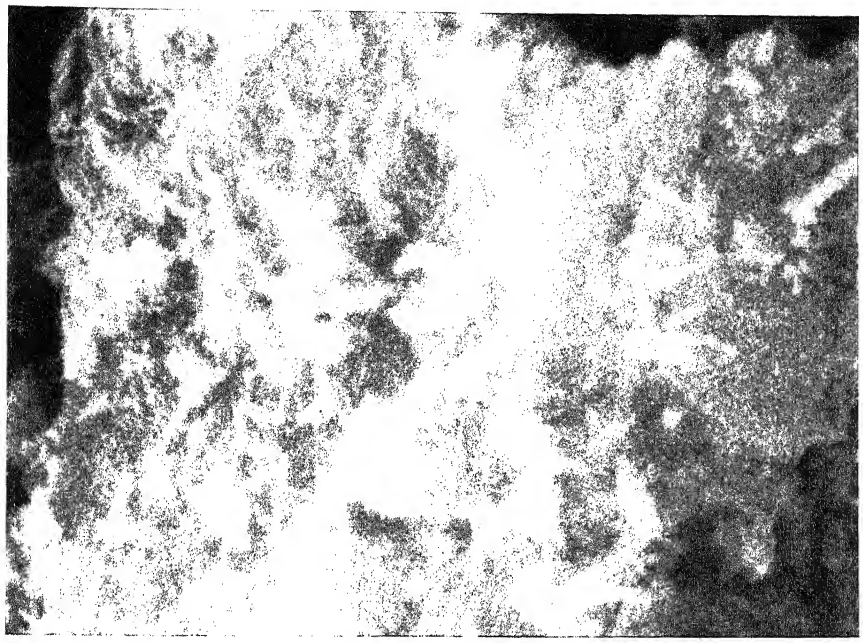

Fig. 4.4(c). SEM micrograph of the double arrow marked particle in Fig. 4.4(a), X20000, showing highly porous cloudy structure.

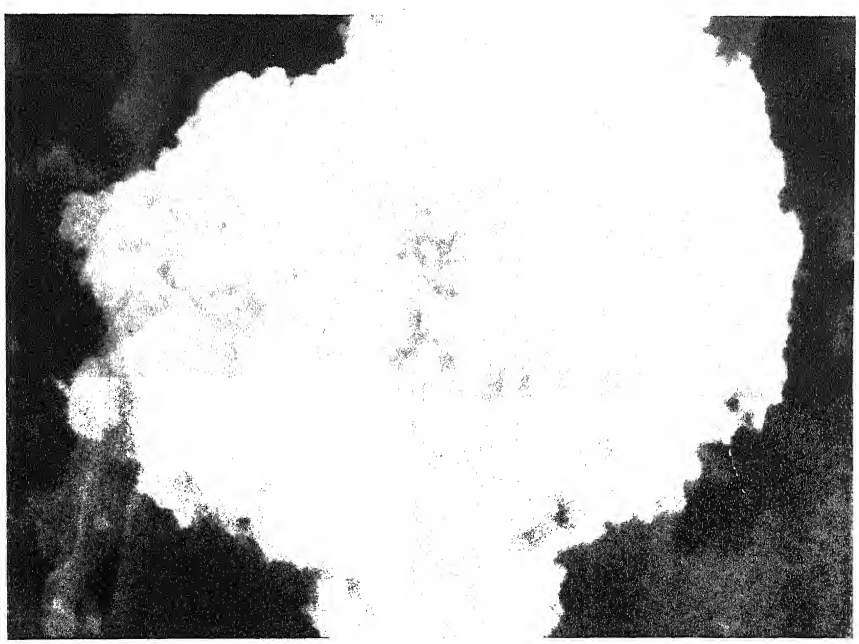

Fig. 4.4(d). SEM micrograph of the sample heat treated at 800°C, X10000, showing irregular particles with rounded shapes but no needles and very low porosity.

At low temperature Fe_3O_4 forms, which reduce to FeO at around 700°C which transforms to Fe on further reduction. Up to a temperature of 600°C no nickel bearing mineral or compound has been identified. At temperatures of 700°C and above, where some iron is observed, or nickel iron alloy has also been seen. Perhaps iron, once formed reacts with nickel to form the alloy

$$Ni + Fe \longrightarrow Fe\text{-}Ni.$$

The metallic Ni which is expected to form at least at 600°C, is not observed by the X-ray and other technique since it is present in small quantity. The amount of Fe-Ni alloy formed is however large enough for detection by the x-ray diffraction method.

Effect of Cooling Treatment : The effect of cooling conditions on heat treated ore was also studied. Details of the variables are presented in Table 4.6. The diffractograms of all the samples heat treated at 600°C under similar conditions but with different cooling treatments were found similar. However, the differences between these samples were seen by the ESCA data presented in Table 4.5, and in leaching studies which are discussed in Chapter 5. The Fe(II)/Fe(III) ratio increases in the order,

Untreated Ore < Aircooled < Fast cooled < Slow cooled < Inert gas cooled samples.

TABLE 4.4. X-ray Diffraction Data for Sukinda Laterite Ore Heat Treated in Hydrogen-Water (60/40 v/v) Mixture for 3 Hours.

S.No.	d, Å	$(2\theta_{Fe})^{\circ}$	hkl	Untreated		200°C		400°C		600°C		700°C		800°C	
				I/I_{max}	Component	I/I_{max}	Component	I/I_{max}	Component	I/I_{max}	Component	I/I_{max}	Component	I/I_{max}	Component
1	2	3	4	5	6	7	8	9	10	11	12	13	14	15	16
1	4.98	22.4	002	0.148	α-FeOOH	-	-	-	-	-	-	-	-	-	-
2	4.19	26.7	011	1.0	α-FeOOH	0.755	α-FeOOH	-	-	-	-	-	-	-	-
3	3.39	33.15	-	0.141	α-FeOOH	-	-	-	-	-	-	-	-	-	-
4	2.94	38.40	220	-	-	-	-	0.282	Fe_3O_4	0.253	Fe_3O_4	0.254	Fe_3O_4	0.314	Fe_3O_4
5	2.91	38.8	-	-	-	-	-	-	-	-	-	-	-	-	-
6	2.76	41.0	104	-	-	-	-	-	-	-	-	-	-	-	-
7	2.70	41.95	013	0.498	α-FeOOH	0.511	α-FeOOH	-	-	-	-	-	-	-	-
8	2.59	43.95	102	0.262	α-FeOOH	0.311	α-FeOOH	-	-	-	-	-	-	-	-
9	2.50	45.65	110	-	-	-	-	1.0	Fe_3O_4	1.0	Fe_3O_4	1.0	Fe_3O_4	0.974	Fe_3O_4
10	2.45	46.5	111	0.778	α-FeOOH	1.0	α-FeOOH	-	-	-	-	-	-	-	-
11	2.26	50.8	112, 103	0.218	α-FeOOH	0.244	α-FeOOH	-	-	-	-	-	-	-	-
12	2.20	52.2	113	0.250	α FeOOH	0.288	α-FeOOH	-	-	-	-	0.236	FeO	-	-
13	2.15	53.4	-	-	-	-	-	-	-			-	-	-	-
14	2.08	55.3	400	-	-	-	-	0.315	Fe_3O_4	0.368	Fe_3O_4	0.336	Fe_3O_4	0.288	Fe_3O_4

...Contd.

1	2	3	4	5	6	7	8	9	10	11	12	13	14	15	16
15	2.06	56.2	111	-	-	-	-	-	-	-	-	0.261	FeNi	0.456	FeNi
16	2.03	57.35	110	-	-	-	-	-	-	-	-	0.137	α-Fe	1.000	α-Fe
17	1.78	65.90	002	-	-	-	-	-	-	-	-	0.120	FeNi	0.183	FeNi
18	1.72	68.35	122	0.323	α-FeOOH	0.477	α-FeOOH	-	-	-	-	-	-	-	-
19	1.71	69.20	422	-	-	-	-	0.118	Fe_3O_4	0.103	Fe_3O_4	0.135	Fe_3O_4	0.111	Fe_3O_4
20	1.69	69.80	116	-	-	-	-	-	-	-	-	-	-	-	-
21	1.60	74.6	333, 511	-	-	-	-	0.131	Fe_3O_4	0.276	Fe_3O_4	0.313	Fe_3O_4	0.327	Fe_3O_4
22	1.58	75.25	-	-	-	-	-	-	-	-	-	-	-	-	-
23	1.56	76.65	115	0.214	α-FeOOH	0.244	α-FeOOH	-	-	-	-	-	-	-	-
24	1.50	80.1	200	0.175	α-FeOOH	0.266	α-FeOOH	-	-	-	-	0.164	FeO	-	-
25	1.48	81.5	-	-	-	-	-	0.552	Fe_3O_4	0.506	Fe_3O_4	0.478	Fe_3O_4	0.425	Fe_3O_4
26	1.45	83.5	202	0.177	α-FeOOH	0.277	α-FeOOH	-	-	-	-	-	-	-	-
27	1.43	85.35	-	-	-	-	-	-	-	-	-	-	-	0.144	α-Fe
28	1.318	94.45	132, 213	-	-	0.173	α-FeOOH	-	-	-	-	-	-	-	-

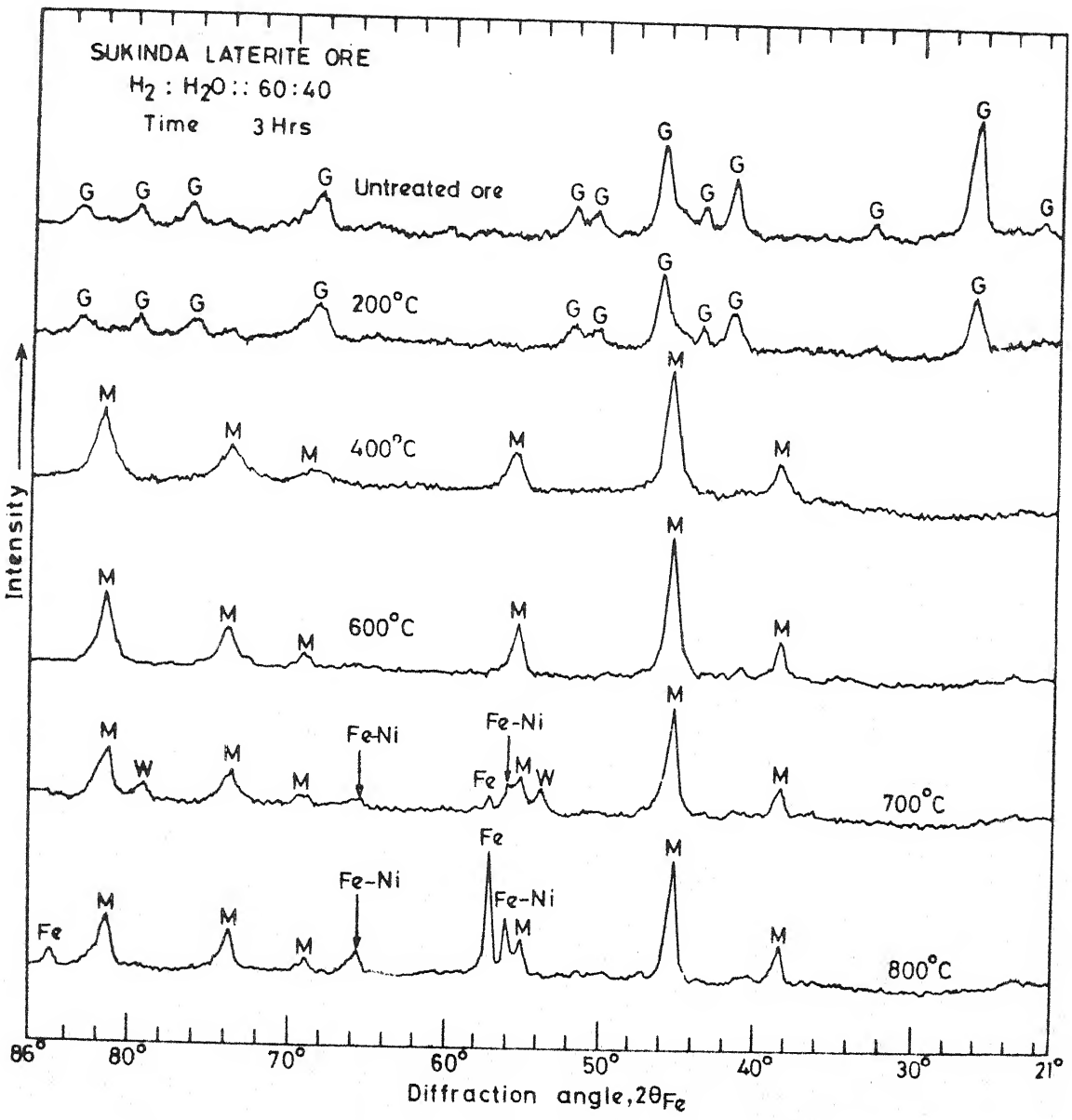

Fig. 4.2. X-ray diffraction pattern for the ore and heat treated samples of Sukinda Laterite.

G : Goethite
Fe: Iron
W : Wustite.
M : Magnetite
Fe-Ni: Iron-Nickel Alloy

TABLE 4.5. Binding Energies, Peak Area and Area Ratio for Fe(II) and Fe(III) as Obtained by ESCA for $Fe2P_3$ Electrons.

Cooling Treatment	Pre-treatment Temp., °C	P_0	P_1	P_2	E_0* eV	E_1 eV	E_2 eV	A_0*	A_1 Fe(III)	A_2 Fe(II)	$\frac{A_2}{A_1}$ or Fe(II)/Fe(III)
Ni Ore	-	-	37.0	51.5	-	712.10	709.80	-	23.52	23.94	1.02
Air cooled	600	-	40.0	53.5	-	711.60	709.45	-	23.65	23.39	0.99
Fast cooled	600	-	35.0	55.0	-	712.40	709.25	-	19.26	34.08	1.77
Slow cooled	600	-	34.5	55.5	-	712.50	709.15	-	16.065	38.05	2.37
Inert gas cooled	600	23.0	36.0	53.0	714.35	712.25	709.55	3.12	12.295	41.68	3.39
Slow cooled	800	-	35.5	56.5	-	712.35	709.00	-	7.628	41.18	5.40

*$E_i = 722 - (P_i \times \delta E) - W.F.$, in eV

where $\delta E = 0.1597$ eV

and W.F. = 4.3 eV (work function)

**A_i is peak area in arbitrary units.

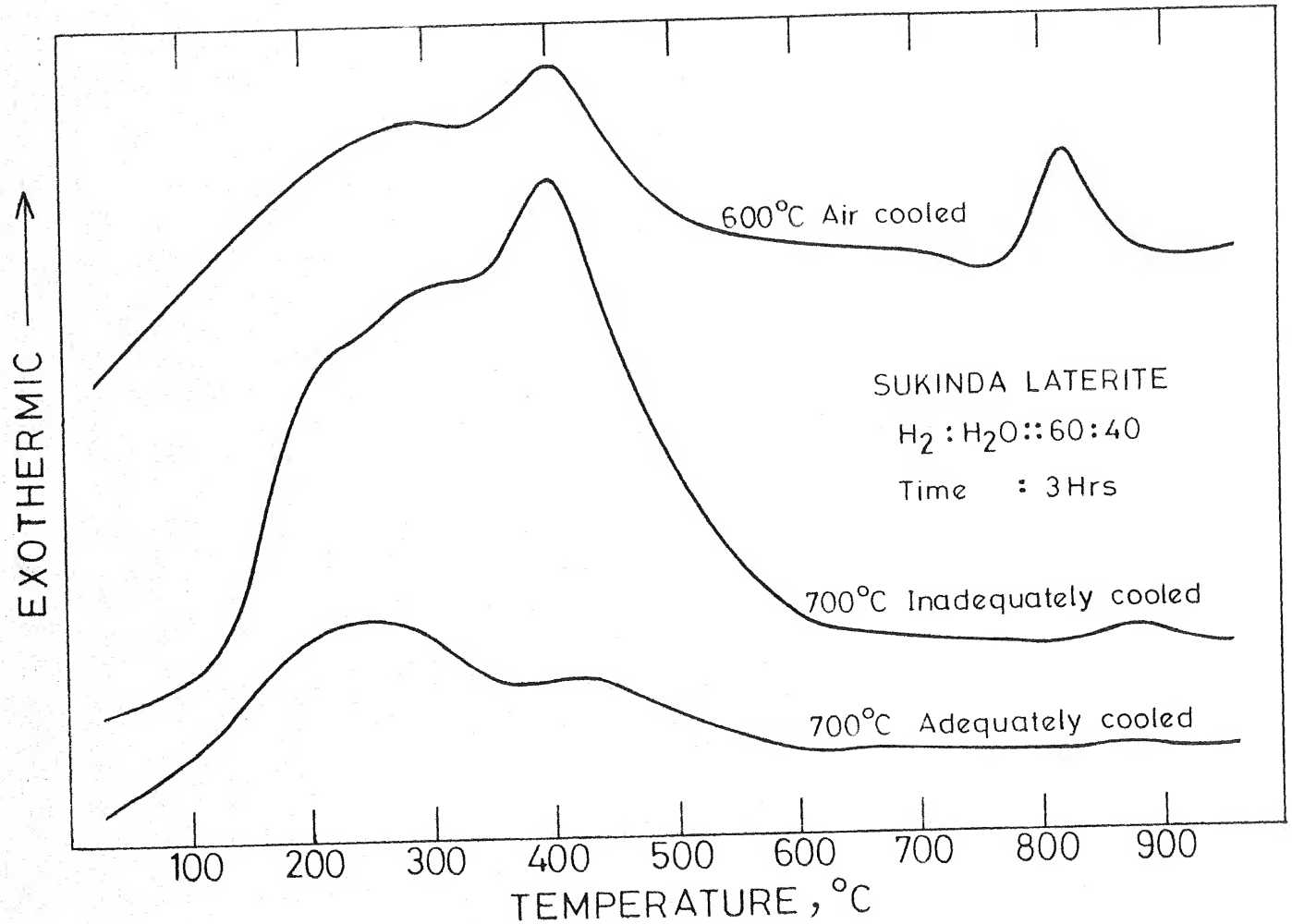

Fig. 4.5. DTA curves for differently heat treated samples with various cooling treatments.

The surface of the air cooled sample gets oxidized to Fe_2O_3 and in this way it is perhaps similar to the untreated ore. The Fe(II)/Fe(III) ratio being same for the untreated and the air cooled samples indicate that the gel type of material believed to be present is a silicate containing ferrous ions which does not react at 600°C. The higher Fe(II)/Fe(III) ratio in fast cooled sample is because reoxidation of the ore is limited. Slow cooling gives still higher Fe(II)/Fe(III) ratio indicating still further decrease in reoxidation of the ore. The maximum Fe(II)/Fe(III) ratio was obtained for the sample cooled in inert atmosphere which allows very little reoxidation. The two ESCA plots in Figures 4.6 and 4.7 for the air cooled and inert gas cooled samples present a more contrasting difference between the two. Inert gas cooled sample gives a three peak function. Though the smallest peak marked U could not be identified yet it is real and seems to be for an unknown phase. The Fe(II)/Fe(III) ratio obtained from the three peak plot matches the value expected from other studies whereas Fe(II)/Fe(III) ratio from the two peak plot did not match the result. All other samples gave only two peak plot similar to the one shown in Figure 4.6 for air cooled sample, with varying peak area.

The effect of cooling environment on the ore heat treated at 700°C was seen in X-ray diffraction studies. The X-ray diffraction pattern in the range 10-50 and 60-100° were

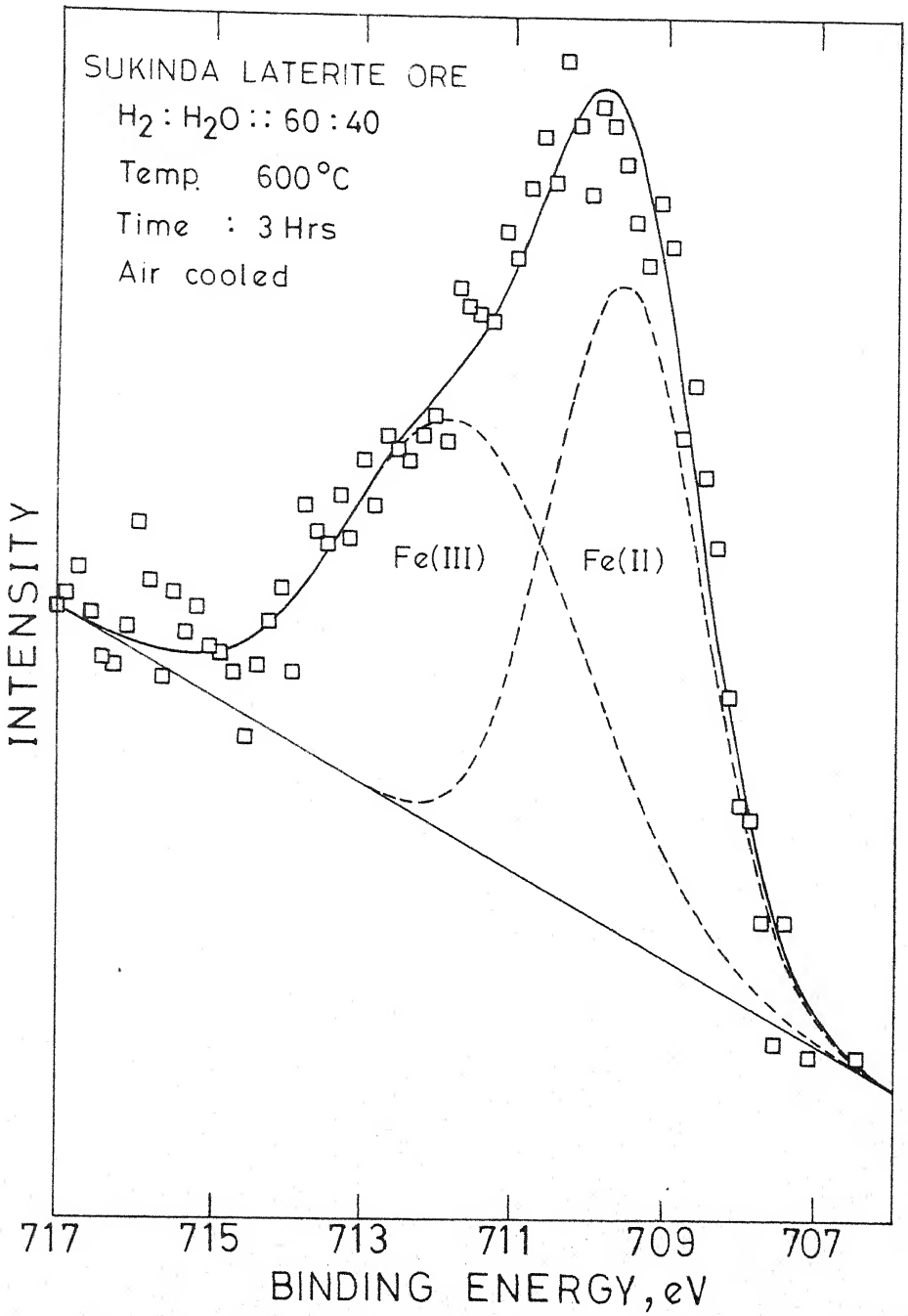

Fig. 4.6. ESCA curves for Fe(II) and Fe(III) in the heat treated sample.

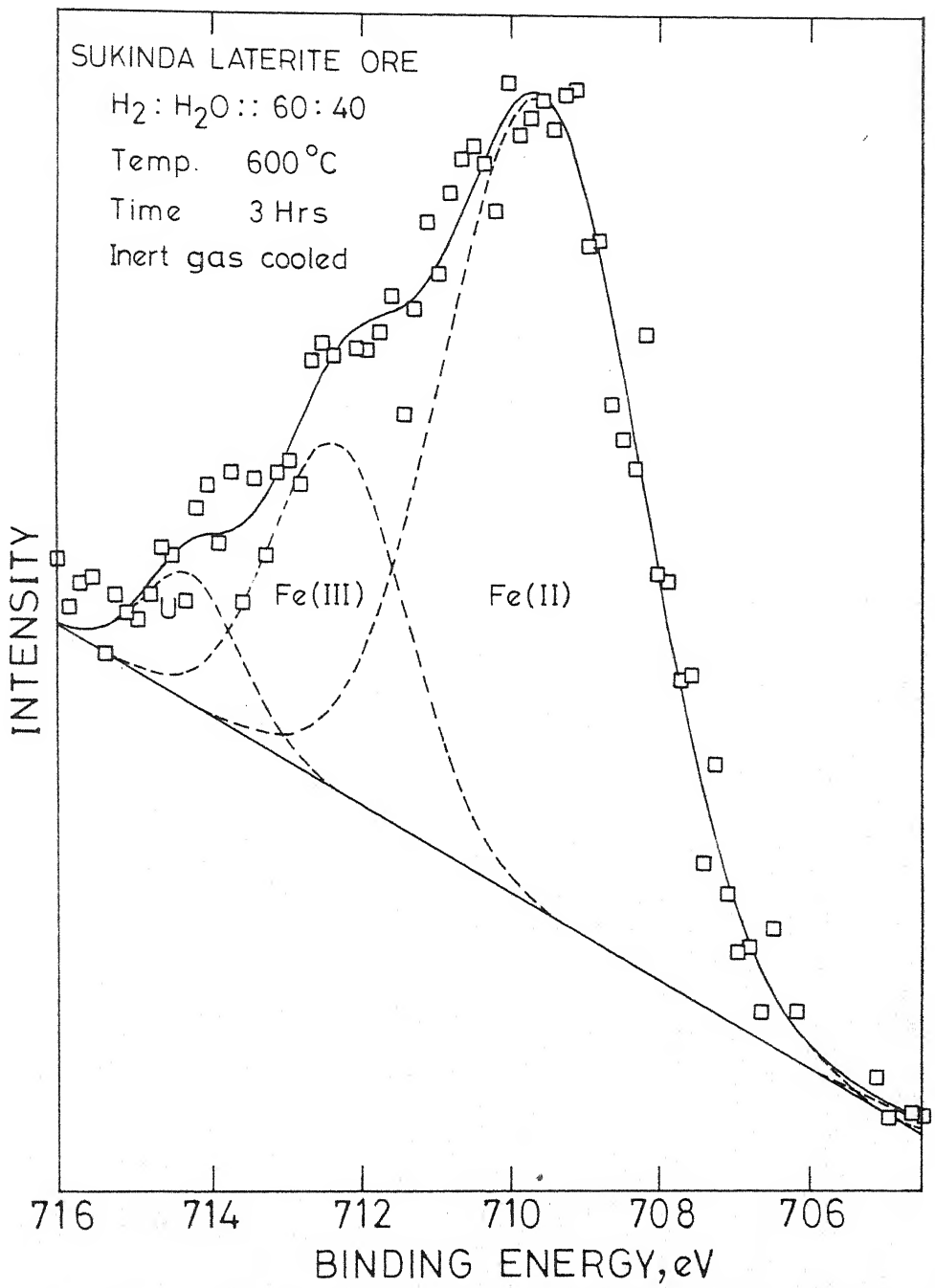

Fig. 4.7. ESCA curves for FeII, FeIII and an unknown phase in the heat treated samples.

identical. However, they were different in the range 50-60° and are presented in Figure 4.8 with corresponding data in Table 4.7. Inadequate cooling resulted in lower FeO and higher α-Fe and Fe-Ni than that obtained from complete cooling. FeO may have transformed to Fe_3O_4. The air cooling gave lower α-Fe and Fe-Ni transformed to Fe_3O_4 and $NiFe_2O_4$. DTA plots in figure 4.5 also indicated lower FeO and higher Fe_3O_4 for inadequately cooled samples than that obtained for complete cooling; thus supporting the view that inadequate cooling may leave the sample hot enough to reoxidise when brought out in the air. Transmission electron microscopic studies were also carried out for samples heat treated at 600°C and cooled in air and inert atmosphere. Though the samples reacted with water at the time of dispersion and formed different phases they were observed to be of widely different characteristics such as in shape and structure. These studies suggest that major change occurred during cooling treatment which affected the leaching behaviour as discussed in the next chapter.

TABLE 4.6. Effect of Cooling Conditions on the Heat Treated Samples of Sukinda Laterite Ore.

Cooling Treatment	Roasting Temp.°C	Cooling Atmosphere (Time in minutes)	DTA* peaks Temp.°C	Constituent Transforming	Fe(II)/Fe(III) (from ESCA)
Ni Ore	-	-	312	α-FeOOH	1.02
Air cooled	600	Air (60)	298 400 820	FeO Fe_3O_4 Fe_3O_4	0.99
Fast cooled	600	H_2+H_2O (60)	-	-	1.77
Slow cooled	600	H_2+H_2O (960)	-	-	2.37
Inert gas cooled	600	N_2 (60)	-	-	3.39
Air cooled	700	Air (60)	-	-	-
Inadequately cooled	700	N_2 (60)	220 295 400 840	FeO FeO Fe_3O_4 Fe_3O_4	-
Adequately cooled	700	N_2 (75)	265 420 840	FeO Fe_3O_4 Fe_3O_4	-
Slow cooled	800	H_2+H_2O (1200)	-	-	5.40

*Data compared with that given in Ref. 41.

TABLE 4.7. X-ray Diffraction Data for Sukinda Laterite Ore Heat Treated at 700°C in H_2-H_2O Mixture and Cooled Under Different Conditions.

d, Å	$(2\theta_{Fe})^{\circ}$	hkl	Inadequately cooled		Adequately cooled		Air cooled	
			I/I_{max}	Component	I/I_{max}	Component	I/I_{max}	Component
2.13	53.90	200	0.176	FeO	0.236	FeO	-	-
2.09	55.20	400	0.352	Fe_3O_4	0.336	Fe_3O_4	-	-
2.07	55.80	400	-	-	-	-	0.259	$NiFe_2O_4$ + Fe_3O_4
2.06	56.10	111	0.615	Fe-Ni	0.261	Fe-Ni	0.260	Fe-Ni
2.02	57.35	110	0.890	α-Fe	0.137	α-Fe	0.410	α-Fe

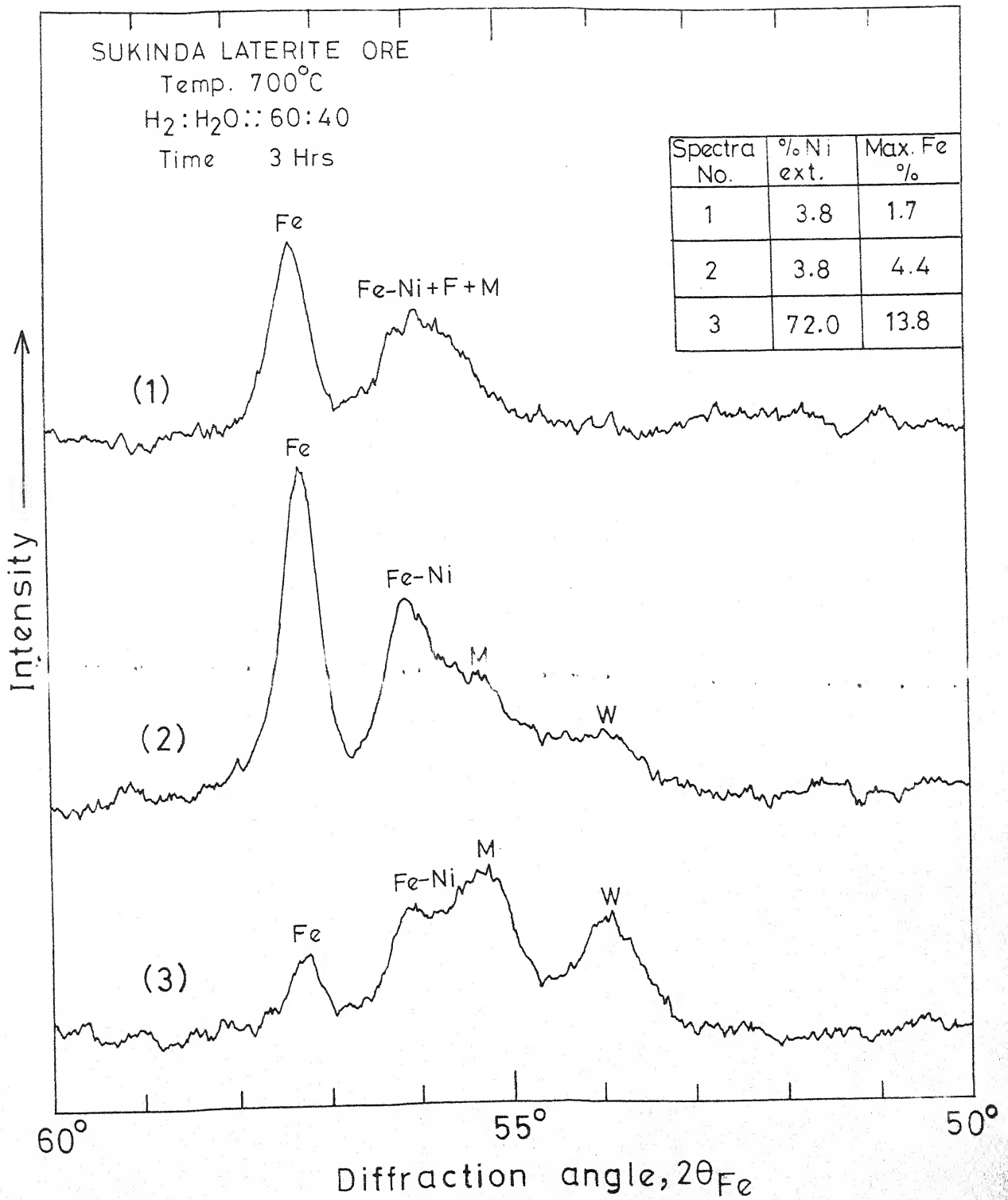

Fig. 4.8: X-ray diffraction patterns for heat treated samples with various cooling treatments.

CHAPTER 5

LEACHING IN AMMONIUM CARBONATE SOLUTIONS AFTER REDUCTION ROASTING

5.1 Introduction

Based on earlier investigations which are reviewed in Chapter 2 the oxide nickel in the ore must be reduced to metallic state to make it soluble. At the same time reduction of iron oxides to lower oxides and metal must be minimised to decrease the amount of iron dissolved. The dissolution of nickel and iron is idealised in the following equation

$$FeNi + O_2 + 8NH_3 + 3CO_2 + H_2O = Ni(NH_3)_6^{++} + Fe^{++} + 2NH_4^+ + 3O_3^=$$

Fe^{++} ions may oxidise to Fe^{+++} ions in the presence of oxygen which may precipitate as ferric hydroxide. The ferric hydroxide may deposit mainly on the ore particle and the walls of the reactor.

$$4Fe^{++} + O_2 + 2H_2O + 8OH^- = 4Fe(OH)_3$$

In this chapter the effect of various variables of roasting, discussed in Chapter 4, on the leaching behaviour of the reduced ore is presented.

5.2 Procedure

The ore heat treated in hydrogen-water mixture (60/40 by volume) was used for leaching. The leaching was carried out in a double walled glass vessel along with a magnetic stirrer used for agitation. Water from a constant temperature bath was circulated through the double wall to maintain a temperature of 40°C. The vessel was closed with a perspex cover with openings for a thermometer, a gas inlet and a tube for withdrawal of samples for analysis. Unless otherwise mentioned 400 ml of one molar ammonium carbonate solution with 2 gm of heat treated ore was used. Ten ml of the slurry sample was withdrawn at preset time intervals and the suspension was filtered. The filtrate was analysed for nickel by spectrophotometric method described in Appendix I. A separate sample was taken for iron analysis. The filtrate was diluted with 5 ml of 60 percent HCl to prevent precipitation of ferric hydroxide. Titration methods for determination of Fe^{2+} and Fe^{3+} are described in Appendix I.

Data presented in Appendix II. gives the complete details of the variables and the amount of nickel extracted and maximum iron dissolved in ferrous and ferric state.

5.3 Effect of Roasting Temperature

Ore sample reduced at 400, 600, 700 and 800°C were leached and the relative extraction, defined as the ratio of

the amount of nickel extracted at a given time to the maximum nickel extracted, is plotted as a function of time in Figure 5.1. The extraction from the ore reduced at 400°C is too small and has been excluded from the figure. Although the amount of nickel extracted at large times, $(Ni^{2+})_{t\to\infty}$, increases with roasting temperature the kinetic data shows that the relative extraction at any given time is larger for lower temperatures. The decrease in the extraction seems to be the effect of sintering. Surface area measurements on samples heated in an inert atmosphere discussed in Chapter 4 confirms sintering. At higher reduction temperatures, more iron is solubilized and the nickel extraction also increases. At these temperatures, Fe_3O_4 is reduced to FeO and Fe. Metallic Ni and Fe formed as a product of reduction give nickel-iron alloy when local concentration of Ni is increased, Fe-Ni alloy has been observed at a temperature of 700 and 800°C but not at 600°C where Fe is not the product of reduction. In ammoniacal solutions Fe and FeO go into the solution as ferrous ammine complex which in the presence of oxygen oxidises to ferric and precipitates as ferric hydroxide. The iron in solution therefore first increases and then decreases with time. The maximum iron in solution is taken as a measure of the relative amount of iron present as soluble iron. In the initial stages of dissolution the solubilization of iron is in the order 600 < 800 < 700°C

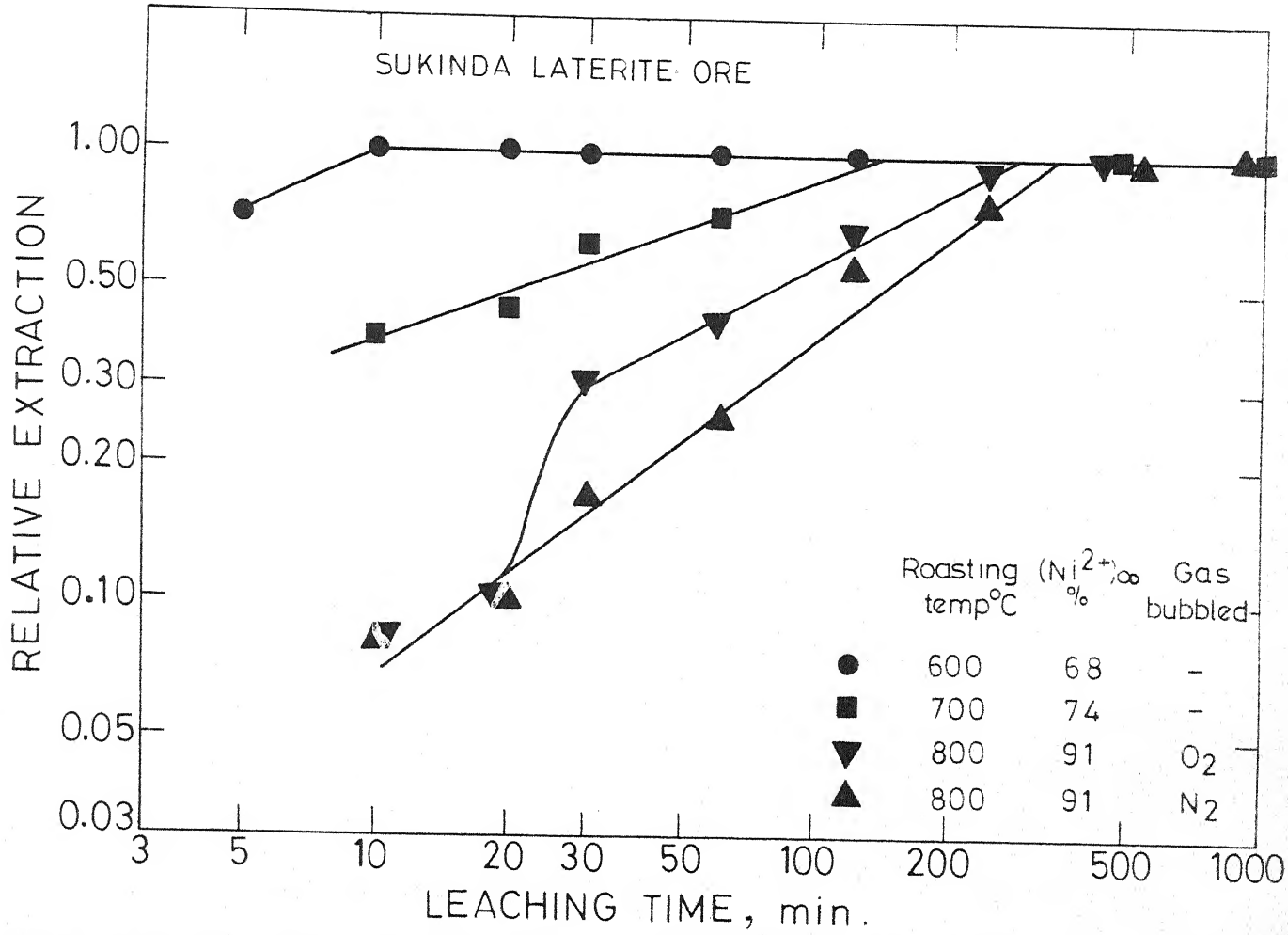

Fig. 5.1. Relative extraction as a function of time at different heat treatment temperatures and gas bubbling during leaching.

which indicates that the dissolution rate for the reduced ore components is in the order $FeO > Fe > Fe_3O_4$.

The Fe/Ni ratios as a function of time, presented in Table 5.1, show that the Fe/Ni ratio for reduction at 800°C is greater than that at 700°C and much greater than that at 600°C in the initial period. The Fe/Ni value takes about 60 to 120 minutes to reach a limiting value for all the three heat treatment temperatures. But even during the period iron dissolution is fast, the Fe/Ni ratio continues to go down from an initial maximum. This indicates that initially iron rich component, i.e. Fe and FeO are dissolved much faster followed by dissolution of a nickel containing constituent.

5.4 Effect of Cooling Conditions

Unless stated otherwise the cooling procedure followed in this study, was to transfer the sample boat after the heat treatment to the furnace-end where the temperature was about 250°C and leave it there for five minutes. The sample was then transferred to the exit-end of the reaction tube and allowed to cool for preset time period without opening the tube. Thereafter the sample was transferred to the leaching vessel for nickel extraction. At 600°C, cooling was done in hydrogen-water mixtures flowing over the sample unless otherwise specified. At 700 and 800°C nitrogen was used as the gas for cooling.

TABLE 5.1. Iron to Nickel ratio as a function of Time for Different Heat Treatment Temperatures.

Time in mts.	Fe/Ni 600°C	Fe/Ni 700°C	Fe/Ni 800°C
0	12.95	16.42	37.9
5	9.53	-	-
10	7.36	8.66	14.99
15	6.72	-	-
20	5.76	2.43	18.11
25	5.44	-	-
30	4.48	1.97	5.35
45	2.24	-	-
60	1.92	-	0.96
90	-	1.31	-
120	1.28	0.64	-
240	-	0.64	0.63
480	-	0.32	-
1080	-	0.32	-

Cooling Time : Four sets of experiments were conducted to see the effect of cooling time on the leaching of the reduced ore at 600°C. Total cooling time was kept at 0 (the sample was quenched directly into the leaching solution), 8, 35 and 60 minutes. From the results presented in Figure 5.2 it is seen that the amount of nickel increases and the amount of maximum iron dissolved decreases with increase in cooling time. The low dissolution of Fe and Ni for the quenched sample seem to have been caused by the reoxidation of the hot sample by air during transfer from the reaction tube into the leaching solution. In other experiments small amount of iron oxidises by the continuously changing equilibrium between iron, hydrogen and oxygen as the temperature decreases. Thermodynamically, oxidation of Fe to FeO and FeO to Fe_3O_4 precedes oxidation of Ni to NiO. Due to this Ni is affected only if the iron oxidation to Fe_3O_4 is complete. If reduced samples are not cooled below 200°C prior to exposure to air the ore may reoxidise with increase in temperature due to exothermic reactions. The reoxidation was observed visually for the sample reduced at 700°C and cooled for 60 minutes prior to exposure to air. The colour of the sample changed from black to red. The sample cooled for 75 minutes did not show such a change. The DTA and X-ray studies confirmed that the sample cooled for 60 minutes contained less FeO and higher Fe_3O_4 than the sample cooled

for 75 minutes. This affects the extractability of nickel as seen in the leaching results. The former gave 3.8 percent nickel extraction whereas the latter gave 72.0 percent nickel. Thus controlled cooling of the roast may be advantageous in obtaining high nickel recoveries at relatively lesser solubilization of iron. The dissolved iron which is present in the ferrous state oxidises to ferric state in the presence of oxygen and precipitates out as ferric oxide or hydroxide.

Cooling Atmosphere : Cooling was done in different atmospheres to determine their effect on the leaching behaviour. The fast-cooled sample was prepared by transferring the boat with the help of a thin wire to the exit-end immediately after the heat treatment was complete with H_2-H_2O mixture flowing continuously. The exist-end of the stainless steel reaction tube was rapidly cooled by running tap water. It was observed that the hot boat evaporated some of the condensed water at the exit-end of the tube and decreased the H_2/H_2O ratio in the gas above the sample. The slow-cooled sample was obtained by allowing the sample to cool to 50°C in the furnace itself with roasting gas flowing continuously during the cooling period. The air-cooled sample was prepared by cooling the sample at the exit-end for 5 minutes and then cooled in air for 55 minutes. The inert gas-cooled sample was prepared by cooling the samples

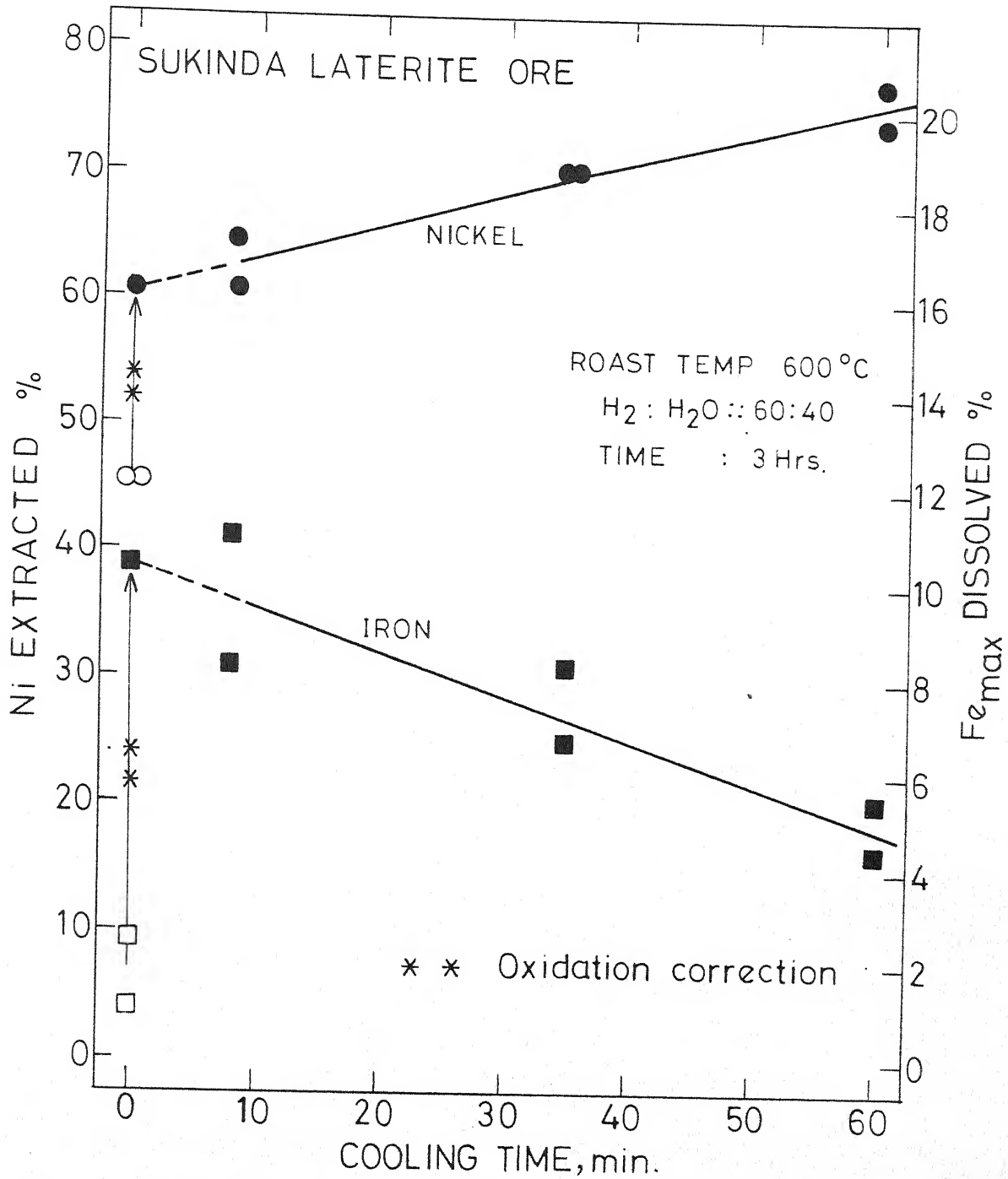

Fig. 5.2. Iron and nickel dissolution curves as a function of cooling time.

in a flow of nitrogen gas for 55 minutes at the exit end of the tube. Cooling for 5 minutes at the furnace end in H_2-H_2O mixture was done before the inert gas was introduced. The quenched-sample was prepared by transferring the hot sample straight from the reaction zone to the leaching solution.

In all cases except inert gas cooling, reoxidation of the reduced sample on cooling is thermodynamically expected. The cooling conditions and corresponding nickel extraction and dissolution of iron are presented in Table 5.2. The amount of metals dissolved for the sample cooled under various conditions follow the order given below.

Fe : Air cooled < Slow cooled < Fast Cooled < Quenched < Inert gas cooled

Ni: Air cooled ≃ Slow cooled < Fast Cooled < Quenched < Inert gas cooled

This shows that the amount of nickel dissolved increases with increase in the amount of soluble iron present in the reduced ore.

The fast cooled sample was observed to have reoxidised possibly because of high H_2O content in the cooling gas. The reoxidation resulted in low nickel extraction and low dissolution of iron. Similar was the result of slow cooling where the lowering of temperature made the thermodynamically more favourable for reoxidation. The air cooling effected reoxidation because of the reaction of the sample with the oxygen from air at high temperature. This also resulted in

low nickel extraction and low iron dissolution. The inert gas cooling gave the highest nickel extraction and iron dissolution because the reoxidising was minimal.

The effect of the cooling atmosphere was studied by ESCA and has been discussed in Chapter 4. The ESCA result presented in Figure 5.3 show that the amount of iron dissolved increases with the Fe(II)/Fe(III) ratio in the reduced samples. These results confirm that the solubilization of iron is maximum when it is present in the ferrous state. This suggests an inverse relation between the extraction of nickel and reoxidation. Hence oxidising components must be absent during cooling.

5.5 Effect of Concentration of the Reducing Gas

To study the effect of change in H_2/H_2O ratio the humidifier bath temperature was varied. The extraction of nickel and iron are plotted as a function of hydrogen content in the H_2-H_2O mixture in Figure 5.4. Extraction of nickel increases significantly for a change in hydrogen content from 50 to 60 percent. On further increase in the H_2 content the nickel extraction does not change appreciably. In the case of dissolution of iron the increase is very large when hydrogen content changes from 50 to 60 percent. With further increase in the H_2 content of the reducing gas, the increase in iron dissolved is relatively small.

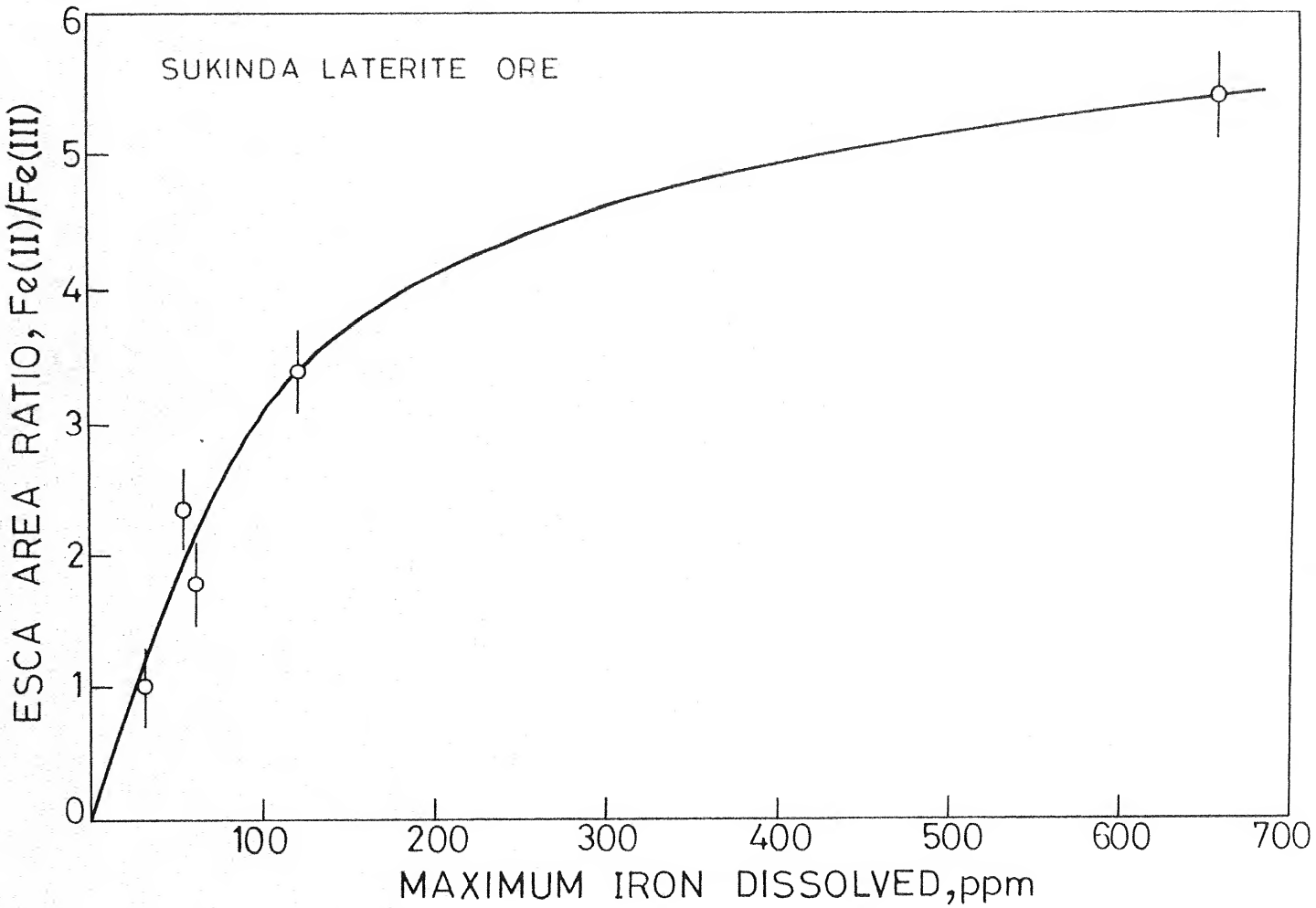

Fig. 5.3. ESCA (FeII/FeIII) ratio as a function of maximum iron dissolved.

TABLE 5.2. Effect of Various Cooling Conditions on the Extractibility of Nickel in the Reducing Roast-Ammonia Leach Process.

Cooling Condition	Roasting Temp. °C	Cooling atmosphere (Time in minutes)	Ni extracted Percentage	Maxm. Fe^{2+} dissolved percentage	Maxm. $Fe_{Tot.}$ dissolved percentage
Air-cooled	600	Air (60)	3.8 3.8	0.55 0.55	1.10 1.10
Slow-cooled	600	H_2+H_2O (960)	5.3 0.0	0.55 0.55	2.20 1.93
Fast cooled	600	H_2+H_2O (60)	4.6 10.0	0.55 0.55	3.86 2.20
Quenched	600	-	45.5 45.5	1.10 1.10	2.76 2.48
Inert gas cooled	600	N_2 (60)	74.0 77.3	3.87 3.31	4.42 5.52
Air cooled	700	Air (60)	3.8 3.8	0.55 1.66	1.66 4.42
Inadequately cooled	700	N_2 (60)	3.8	1.66	4.42
Adequately cooled	700	N_2 (75)	72.0	8.83	13.81
Quenched	800	-	72.0	27.06	32.58
Slow cooled	800	H_2+H_2O(1200)	87.1	19.92	23.72

The results confirm the thermodynamically expected behaviour of the reduction. The reduction of nickel oxide to nickel appears to be complete at H_2/H_2O ratio of 60/40. The amount of FeO and Fe in the reduced ore is expected to increase with decrease in H_2/H_2O ratio, thereby increasing the amount of dissolved iron.

5.6 Effect of Salt Addition and Their Concentration

The effect of additions during roasting of a number of salts, namely, sodium chloride, calcium chloride and magnesium chloride was studied on leaching. All these salts are highly hygroscopic and difficulties were encountered in mixing them thoroughly and uniformly with the ore. To add the salt and ensure uniformity the salt was dried at 120°C in an oven for 5 hours, crushed, ground hot and redried for 2 hours before adding it to a known amount of laterite ore in a sample bottle to approximately give a 6 percent mixture of the salt. The salt composition was brought to 4 percent with ore additions. The salt-ore mixture was diluted by further addition of the ore to give 2, 1 and half a percent mixture. Two grams sample of the mixture heat treated at 600°C for 3 hours in H_2/H_2O mixture was leached in 400 ml of one molar ammonium carbonate solution at 40°C. At the preset time nickel and iron in the solution were determined. The data and the nature of the plots are presented in Figures 5.5 to 5.7.

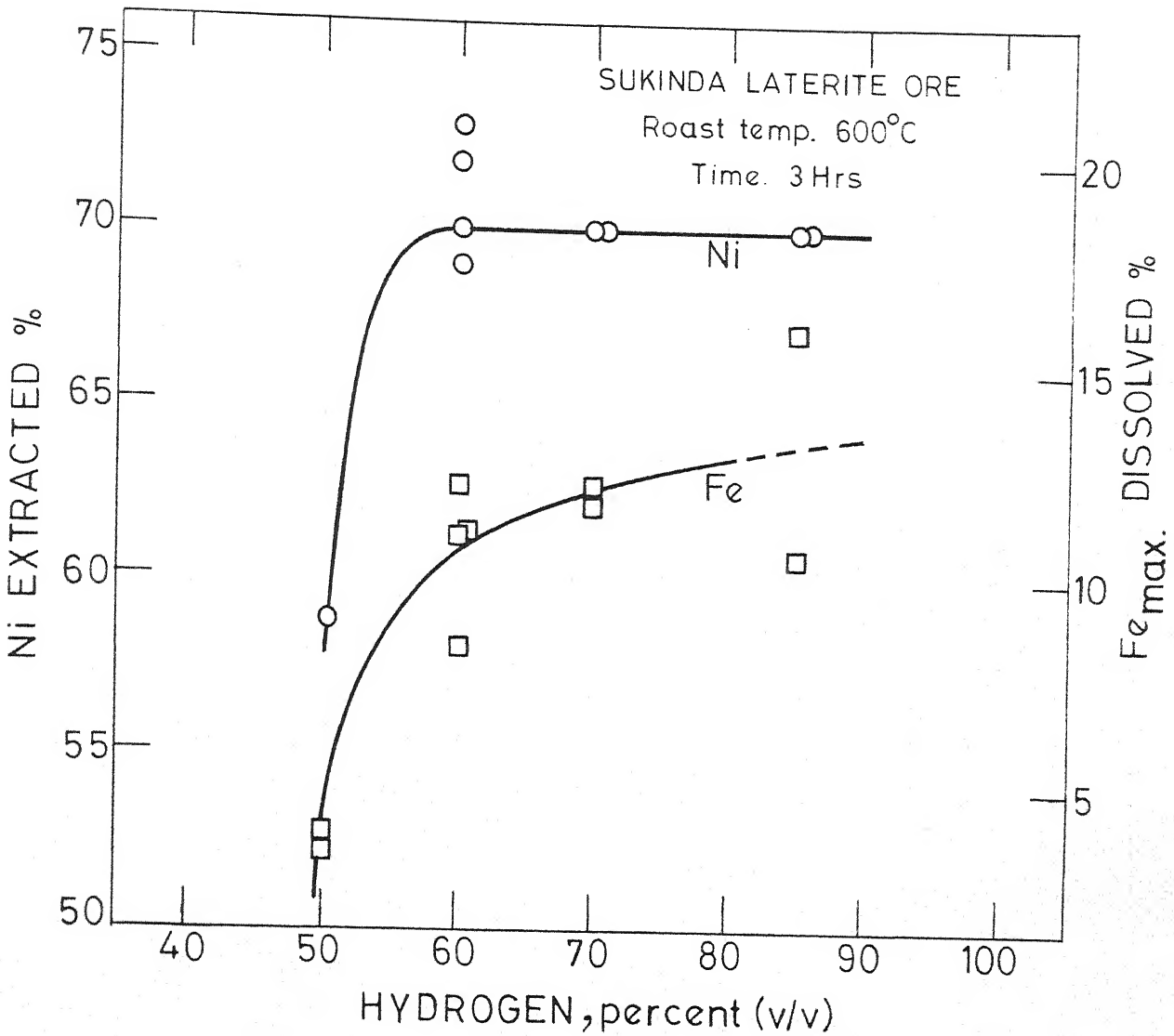

Fig. 5.4. Nickel extraction and iron dissolution as a function of hydrogen concentration in reducing gas mixture.

With increase in salt concentration of NaCl and $CaCl_2$ the nickel extraction first increases reaching a maximum at one percent and then decreases at higher salt concentration as shown in Figure 5.5. Thereafter nickel extraction again increases but very slowly. For $CaCl_2$ iron dissolution follows the same pattern as nickel extraction but in case of NaCl iron dissolution linearly increases from half a percent to 4 percent. This is shown in Figure 5.6. $MgCl_2$ follows a very similar pattern in case of both nickel and iron - first remaining almost constant from one to two percent and then increases up to 4 percent salt addition. Figure 5.7 shows the correlation between the extraction of nickel and solubilization of iron with and without salts. In the absence of salt, and in the presence of $CaCl_2$ and $MgCl_2$ extraction increases linearly with the amount of maximum iron dissolved. The increase in nickel is very small for a large change in iron.

5.7 Phase Changes During Leaching

A study of Figure 5.8 which contains the diffractograms of the untreated ore, the ore heat treated at 800°C in wet hydrogen and that of the leach residue indicates that on roasting all the phases of goethite in the ore get changed to α-Fe, Fe-Ni alloy and Fe_3O_4, as has been discussed in detail in Chapter 4. On leaching, Fe-Ni alloy seem to get

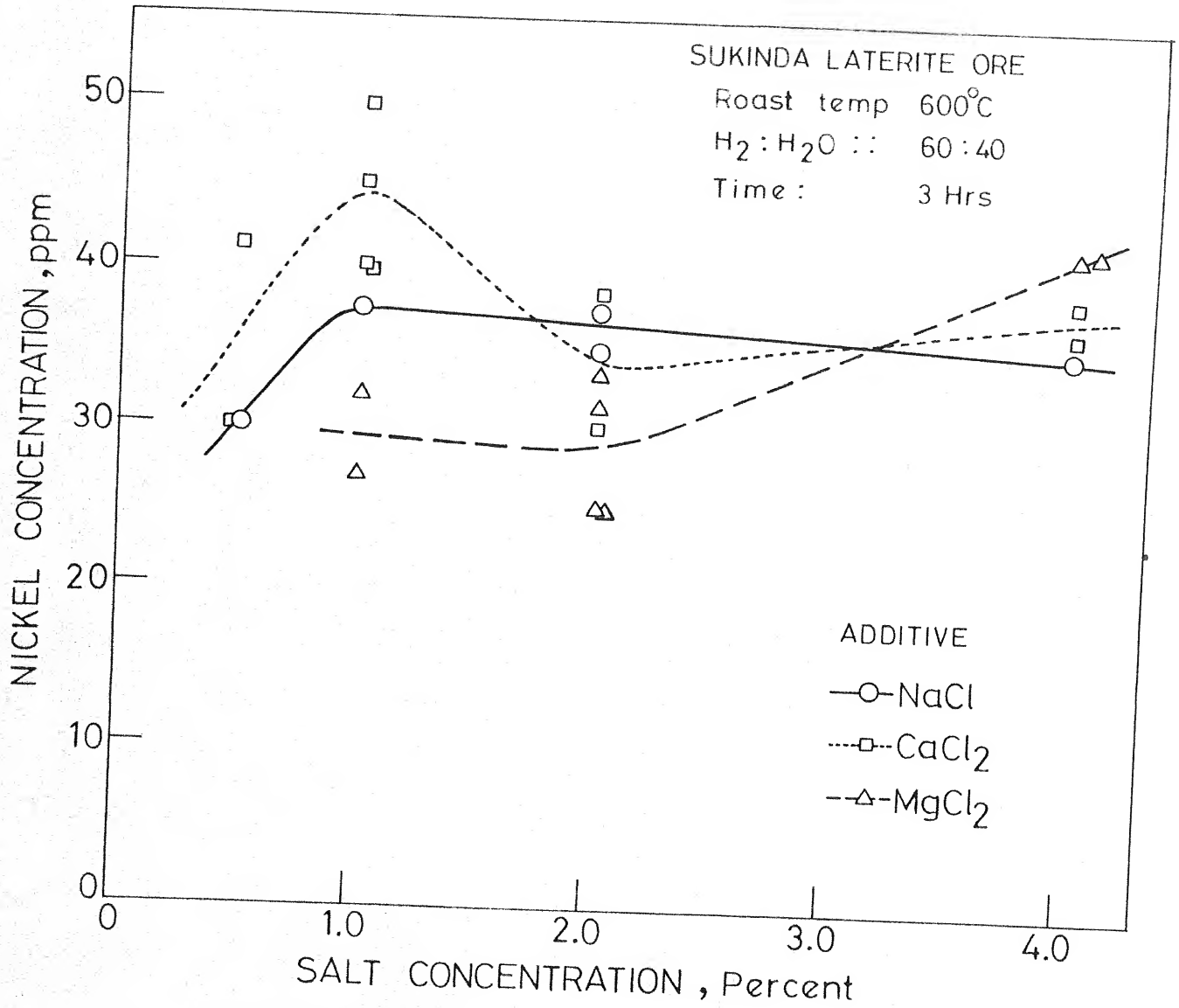

Fig. 5.5. Nickel extracted as a function of salt concentration.

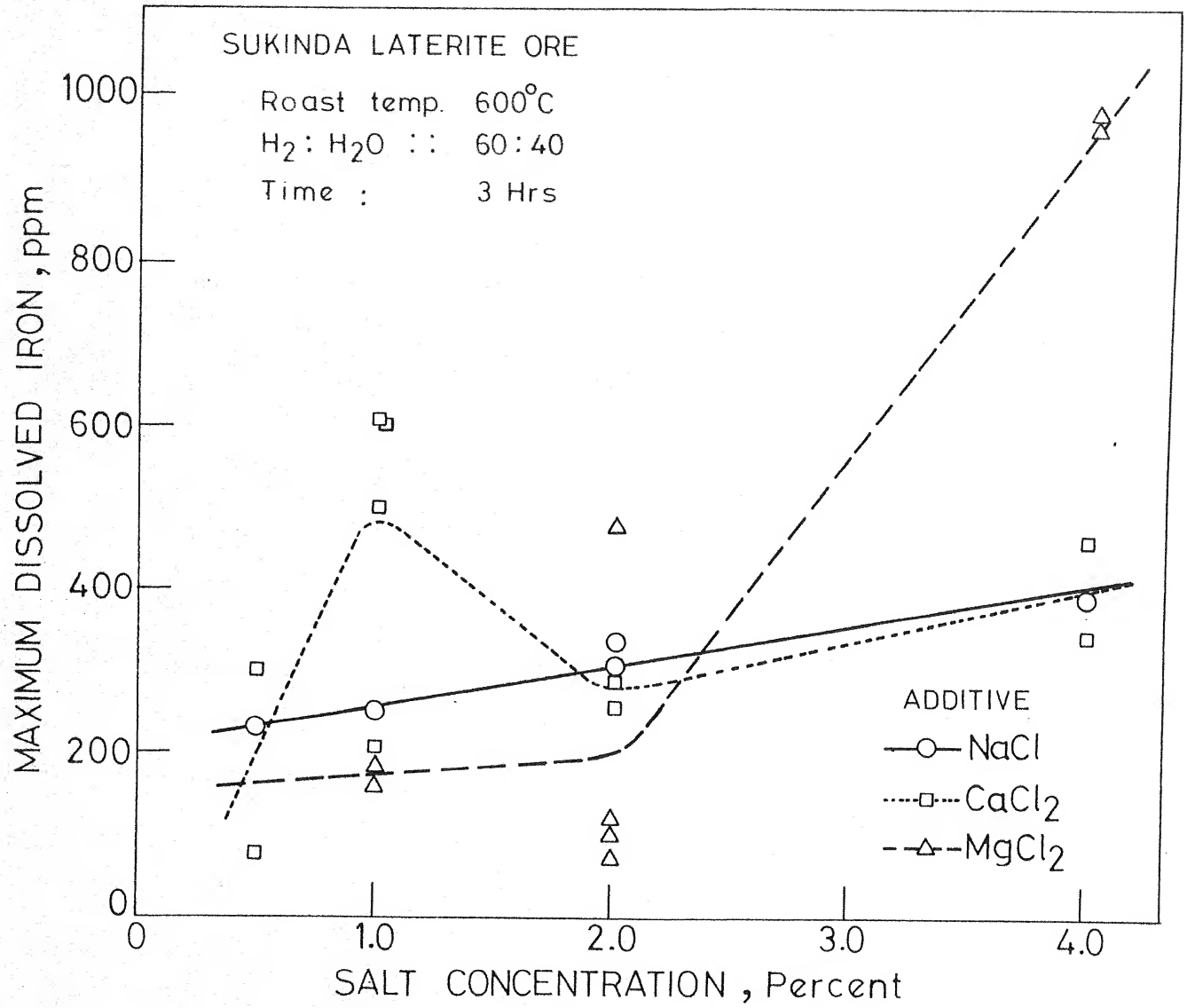

Fig. 5.6. Maximum iron dissolved as a function of salt concentration.

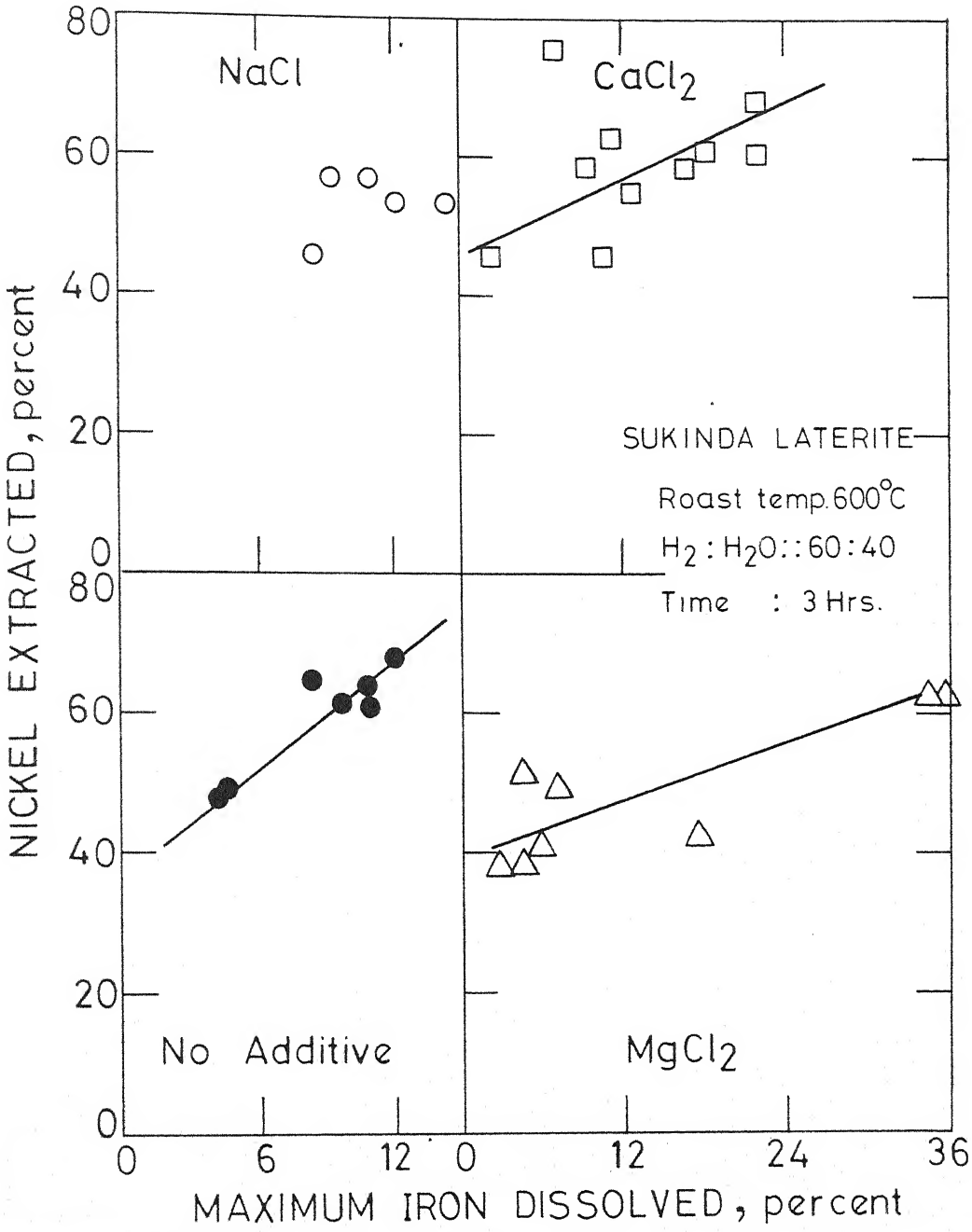

Fig. 5.7. Nickel extracted as a function of maximum iron dissolved with and without salt additions.

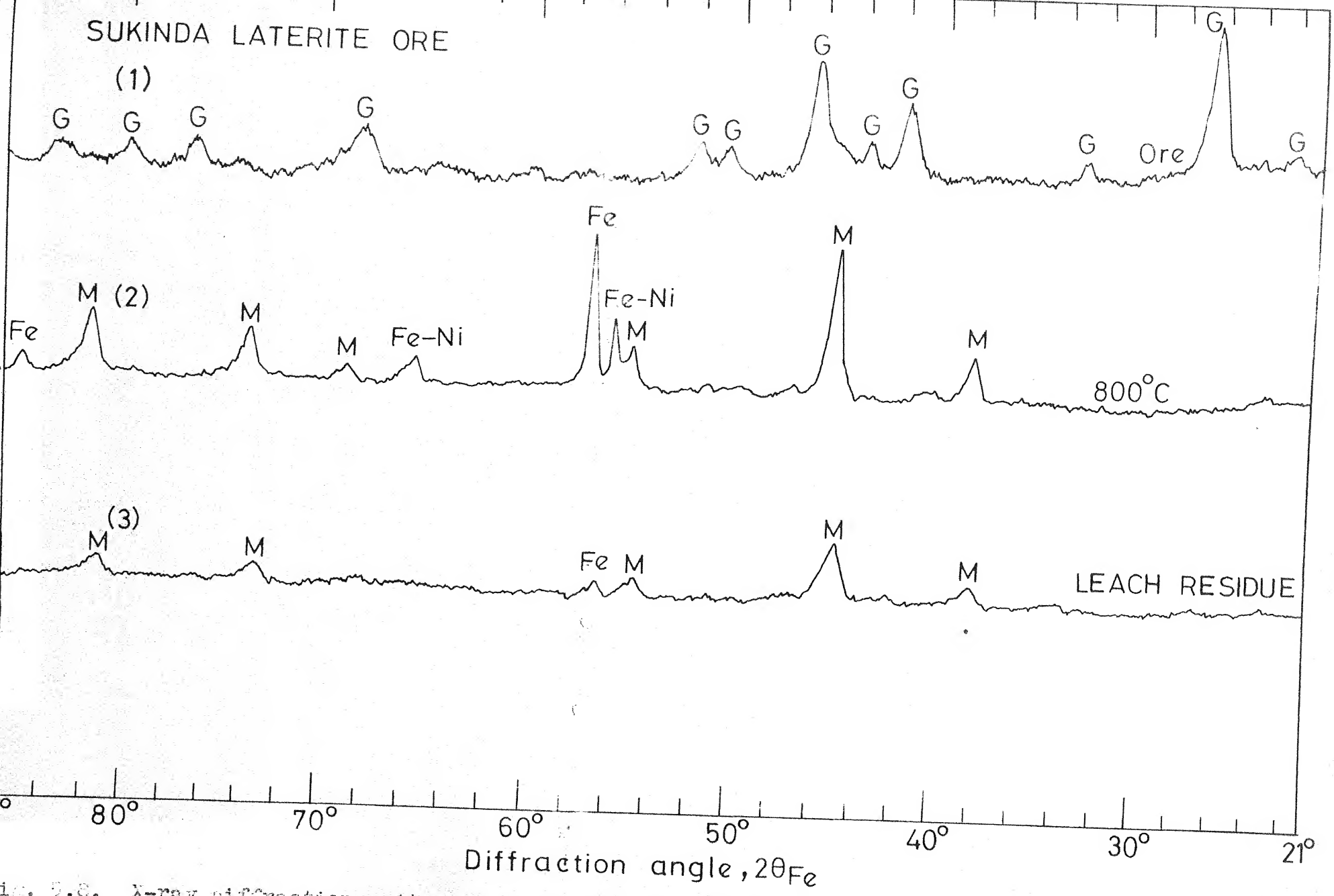

Fig. 5.8. X-ray diffraction pattern for the ore, the sample heat treated at 800°C and the leach residue.

completely dissolved as no peak for this phase is observed in the spectra for the leach residue. Only Fe_3O_4 peaks along with a small peak for α-Fe are seen. The $Fe(OH)_3$ precipitated due to oxidation of Fe(II) to Fe(III) seem to be in amorphous state and does not give X-ray diffraction. However, in electron microscopic studies the amorphous precipitate transforms to Fe_2O_3 in the electron beam and is seen as a mixture of rod and needle shaped opaque particles at lower magnification as shown in Figure 5.9a. These particles have highly porous structure at higher magnification as shown in Figure 5.9b. The diffraction pattern for this particle is presented in Figure 5.9c and the indexing pattern in 5.9d. This is indexed to be a hexagonal system of α-Fe_2O_3. Scanning Electron Micrograph of the leach residue of the sample heat treated at 800°C is presented in Figure 5.10. The micrograph at lower magnification showed a mixture of round and rod shaped particles but at higher magnification the material is seen to be porous with mostly rod type shapes. This may be a mixture of magnetite and ferric hydroxide. It may be compared with the Scanning Electron Micrograph of the ore in Figures 3.2b-e and of the heat treated sample at 800°C in Figure 4.4d to observe the difference.

X-ray diffraction pattern of the leach residue of the ated at 600°C in H_2-H_2O mixture was compared

with that of the sample roasted at the same temperature. No significant difference was observed and all the phases were that of Fe_3O_4 in both cases. This indicates that at 600°C Fe_3O_4 is formed which has very very low dissolution in the leaching solution. But dissolved iron oxidises to give ferric hydroxide which is amorphous and is not seen by X-ray. Also taking high extrability of Ni into consideration for the same sample it may be concluded that at 600°C reduction of NiO→Ni takes place which dissolves very fast in the leaching solution. But further reduction of Fe_3O_4 does not take place at this temperature which leaves Fe_3O_4 as it is, even in the leach residue.

5.8 Miscellaneous

Effect of variation of particle size in the range -30+60 to -140+200 did not significantly effect the extraction of nickel or dissolution of iron.

The influence of drying the ore prior to reduction was determined by comparing the extraction of nickel and iron from ore samples dried at 150°C and 250°C for 7 hours with the undried ore. The nickel and iron extractions were found to be the same after the correction in the weight of the sample for the water loss has been made. The results show that drying the ore upto a temperature of 250°C does not alter the reduction and leaching characteristics of the ore.

(a)

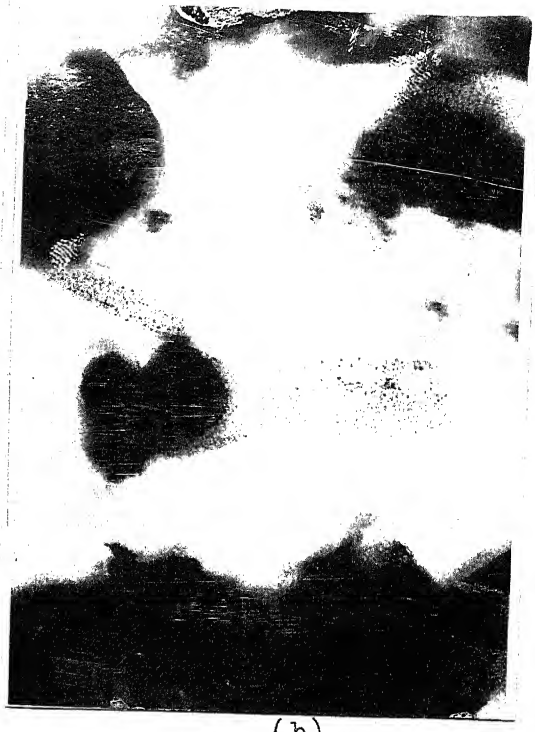

(b)

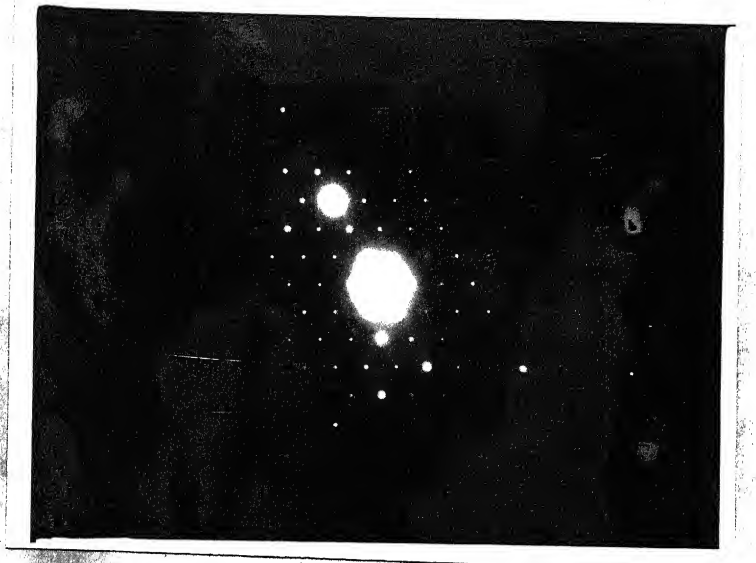

(c)

Fig. 5.9. TEM micrograph of the leach residue of sample heat treated at 800°C showing,
(a) Rod and needle shaped opaque particles, X2200,
(b) Highly porous structure in one of the particles shown in Fig. 5.9(a), X28000, and
(c) Electron Diffraction Pattern of the particle shown in Fig. 5.9(b).

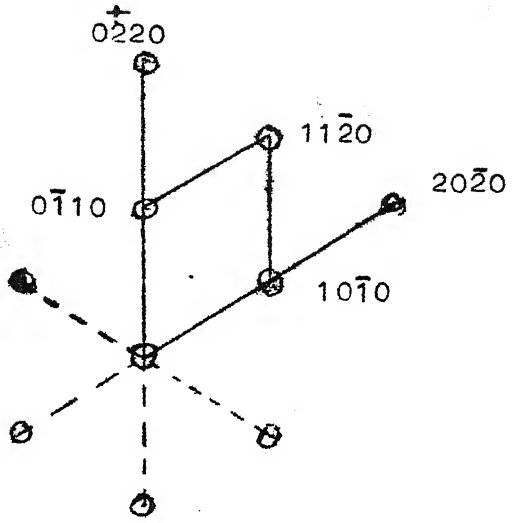

Fig. 5.9(d). Indexing pattern of the Electron Diffraction in Fig. 5.9(c). It is indexed as hexagonal system of α-Fe_2O_3 with a = 5.033.

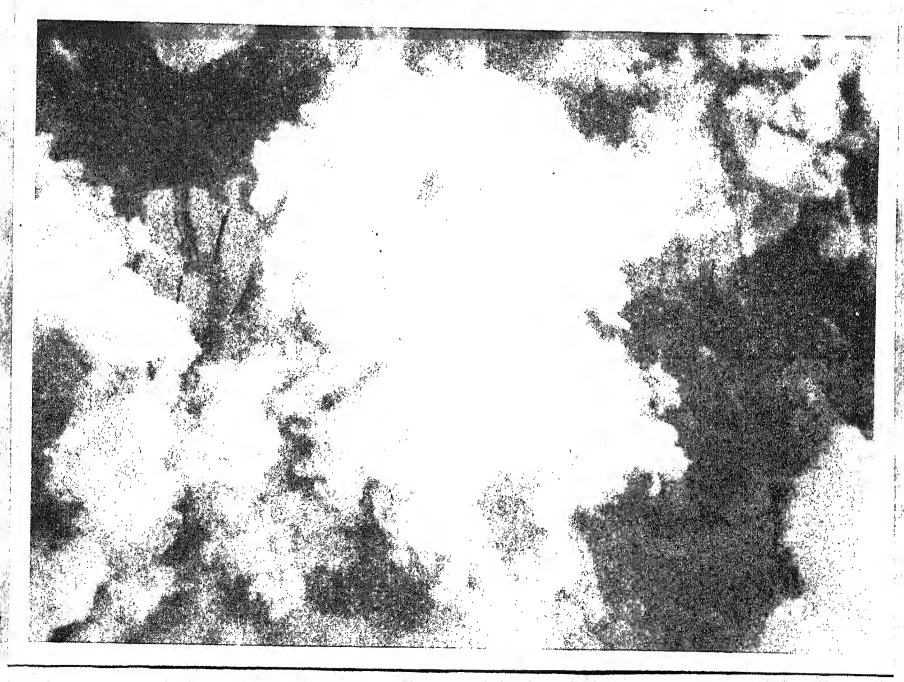

Figure 5.10. SEM micrograph of the Leach residue of the sample heat treated at 800°C, X10000.

CHAPTER 6

CONCLUSIONS

Based on the studies of the Sukinda Laterite ore reported in Chapter 3 the ore characteristics are as follows:

1. The ore is very soft and a weak agglomerate of very fine particles. The particles have high surface area and are highly porous.
2. Nickel is uniformly and finely distributed in the ore. Hence beneficiation of the ore based on selective sizing is not possible.
3. The ore is primarily goethite with iron in Fe(III) state. But surface of the ore contains almost equal amount of Fe(II) and Fe(III). Fe(II) is amorphous and present in gel form. It could not be detected by X-ray and Electron Diffraction techniques but has been seen by ESCA.
4. The goethite in the ore has needle shaped particles which shows highly fibrous structure at high magnification. The rod shaped particles in the ore seem to be hollow cylinders filled with smaller particles.
5. The goethite in the ore undergoes an endothermic transformation at 312^{o}C which indicates that the goethite is in poorly crystallised form; possibly containing some isomorphically substituted impurities.

The effect of heat treatment in argon, dry hydrogen and wet hydrogen was studied by various techniques and is summarized below:

1. Surface area of the particle decreases with increase in heat treatment temperature indicating sintering, which affects the reduction and leaching characteristics of the ore.
2. The ore transforms to hematite if heated in argon atmosphere at 400 and 600°C. But at 800°C the ore transforms to hematite with a small amount of Fe_3O_4.
3. Pretreatment in dry hydrogen reduces the iron and nickel oxides of the ore and follows the Fe-H-O and Ni-H-O equilibrium conditions. Reduction pattern for heat treatment in hydrogen-water mixture also follows the thermodynamic equilibria.
4. Formation of Fe-Ni alloy in reduction roasting suggests the presence of a separate nickel or iron-nickel mineral but no evidence could be seen. High nickel extraction from those heat treated samples where Fe-Ni alloy are not formed suggests that nickel exists as oxide/hydroxide independent of Fe in Sukinda laterite.
5. Inert cooling atmosphere helps in retaining the reduced phase. Hence the sample must be allowed a critical cooling period to cool the sample to 50°C in inert atmosphere. Even surface oxidation seems to inhibit nickel extraction. Inadequate cooling causes reoxidation of the reduced sample and is accompanied by exothermic reactions.

Based on the leaching studies of the roasted sample in Ammonium carbonate solution following conclusions can be made:

1. Extraction of nickel and dissolution of iron increases with increase in roasting temperature though the rate of extraction of Ni and dissolution of Fe decreases with increase in the roasting temperature.
2. Increase in Ni extraction is generally accompanied by increase in iron dissolution with all salt additions and at all temperatures.
3. Longer cooling time resulted in higher nickel extraction and relatively lower iron dissolution.
4. Hydrogen to water ratio of 60/40 gives the highest nickel extraction and relatively lower iron dissolution. At H_2/H_2O lower than 60/40, both Ni extraction and Fe dissolution are low and at higher than 60/40 Ni extraction remains constant but iron dissolution increases.
5. One percent NaCl and $CaCl_2$ and four percent $MgCl_2$ additions give the maximum nickel extraction and solubilisation of iron for the respective salt additions.
6. The salt additions influence the dissolution of nickel and iron differently which indicates that a high nickel compound may be present in the ore when roasted at $600^{\circ}C$ in H_2/H_2O mixture. This compound gets reduced to an FeNi alloy at higher reducing temperatures of 700 and $800^{\circ}C$.

7. Predrying and change in particle size of the ore does not significantly alter the extraction.

8. The optimum conditions for best extraction results are to reduce NiO to Ni and Fe_2O_3 to Fe_3O_4 and to small amount of FeO. At 600°C when these transformations take place particles retain their highly porous structure which gives faster and better extraction results, that is, high nickel extraction and low iron dissolution at a faster rate.

APPENDIX I

ESTIMATION OF NICKEL, FERROUS AND FERRIC IRON

Preparation of the Sample

(a) Sukinda Laterite : Half a gm of the laterite ore is mixed with 10 ml each of the concentrated HCl, HNO_3 and HF acids in a plastic bottle. The bottle is heated in a boiling water bath for about 4 hours and then 10 ml of $HClO_4$ is added, and heating continued until all solids are dissolved. The solution is quantitatively transferred to a 100 ml volumetric flask by washing the plastic bottle many times and transferring the contents to the 100 ml volumetric flask. By adding distilled water the solution is made up to the mark. This solution is used for estimation of nickel in the ore by the procedure described below.

(b) Leach Solution : As described in Chapter 5 samples are removed from leach solution and filtered separately - one in empty sample bottle and the other in 5 ml of 60 percent HCl solution at preset time. The first filtrate is used for estimation of nickel and the second one for estimation of ferrous and ferric iron by the procedures given below.

Nickel Analysis

Principle : Estimation of nickel is done by preparing a dimethyl glyomine complex of nickel in a medium of ammoniacal

ammonium citrate and by comparing the absorbance of this complex with that of the calibration plot at 530 nm by spectrophotometer.

Procedure : One ml of the sample solution prepared by the procedure (a) or (b) above is taken into a 100 ml vol. flask and 20 ml water and one ml perchloric acid are added to it. It is followed by 10 ml of 50 percent ammonium citrate solution and one ml of 0.1 M iodine solution. After every addition thorough mixing is done and then 20 ml of 0.1 percent dimethyl glyoxime solution is added and solution diluted up to the mark. After thorough mixing the solution is allowed to stand for 5 minutes to complete the complex formation. The clean sample cell is then filled with this solution and after cleaning the outer walls the cell is transferred to the sample box of the already warmed up spectrophotometer. Absorbance at 530 nm is recorded and exact nickel content is known by comparison with the calibration plot.

Estimation of Ferrous Iron in the Leach Solution

Principle : The ferrous solution is acidified and titrated by standard potassium dichromate solution in the presence of an indicator until change in colour is stable.

Procedure : Two ml of the solutions obtained in (a) or (b) above is taken in a conical flask and diluted with 50 ml of 2.5 percent H_2SO_4. 2 ml of syrupy phosphoric acid and

2 drop of diphenylamine indicator are added and thoroughly mixed. This is titrated against standard $K_2Cr_2O_7$ solution until deep blue colour is obtained and persists for 5 minutes. Amount of ferrous Iron is calculated as

1 ml N/10 $K_2Cr_2O_7$ = 0.05585 gm Fe.

Estimation of Ferric Iron in the Leach Solution

Principle : The solution is first completely reduced to ferrous state and then in acid medium is titrated against the standard potassium dichromate solution in the presence of an indicator until change in colour is stable. This gives the value of total iron. Ferric iron is obtained by subtracting ferrous from the total iron.

Procedure : Two ml of the leach solution (already filtered in 5 ml of 60 percent HCl) or the solution of the dissolved ore is taken into a conical flask and heated just to boiling. Freshly prepared stannous chloride solution is added dropwise until the yellow colour completely disappears. One drop of stannous chloride is added to it. The flask is closed and the solution cooled under tap water. 2 drops of 5 percent Mercuric chloride is added to the cooled solution and allowed to stand for 5 minutes. White silky precipitate of mercurous chloride is obtained. 50 ml of 2.5 percent H_2SO_4 and 2 ml of syrupy phosphoric acid followed by 2 drops of diphenyl

amine indicator are added and stirred well. This is titrated against standard $K_2Cr_2O_7$ solution until deep blue colour is obtained and persists for 5 minutes. Amount of total Iron is calculated as

1 ml N/10 $K_2Cr_2O_7$ = 0.05585 gm Fe.

Fe(ic) Iron = Total Fe - Fe(ous) Iron.

TABLE: Data on Ni Extraction and Iron Dissolution and Effect of Variables of Reduction Roast and Ammonia Leaching on Sukinda Laterite Ore.

Expt. No.	Ni extracted %	Max. Fe^{2+} dissolved %	Max. Fe_{Tot} dissolved %	Heat treatment Temp. °C	H_2/H_2O ratio	Addition salt %	Particle size, mesh	Cooling conditions: Atm.	Cooling conditions: Time (minutes)	Leaching atmosphere	Pre-drying of the Ore
1	2	3	4	5	6	7	8	9	10	11	12
1	63.6	-	-	800	60/40	-	-65+100	N_2	10	Air	-
2	41.7	-	-	"	"	-	"	"	"	"	-
3	50.4	-	-	"	"	-	"	"	"	"	-
4	48.1	-	-	600	"	-	"	"	"	"	-
5	55.7	-	-	"	"	-	"	"	"	"	-
6	58.3	-	-	"	"	-	"	"	"	"	-
7	6.8	-	-	400	"	-	"	"	"	"	-
8	7.6	-	-	"	"	-	"	"	"	"	-
9	75.8	-	-	800	"	-	"	"	"	"	-
10	75.8	-	-	"	"	-	"	"	"	"	-
11	83.5	-	-	"	"	-	"	"	"	"	-
12	75.8	-	-	"	"	-	"	"	"	"	-

...Contd.

Table (Contd.)

1	2	3	4	5	6	7	8	9	10	11	12
13	90.9	-	-	800	60/40	-	-65+100	N_2	10	N_2	-
14	90.9	-	-	"	"	-	"	"	"	O_2	-
15	75.8	-	-	"	"	-	"	"	"	N_2	-
16	56.8	-	9.14	600	"	1 NaCl	"	H_2-H_2O	"	Air	-
17	56.8	-	-	"	"	"	"	"	"	"	-
18	53.0	7.72	12.16	"	"	2 NaCl	"	"	"	"	
19	56.8	6.63	11.03	"	"	"	"	"	"	"	-
20	45.5	4.19	8.37	"	"	0.5NaCl	"	"	"	"	-
21	53.0	8.81	14.34	"	"	4 NaCl	"	"	"	"	-
22	56.8	4.44	7.72	"	"	-	-30+60	"	"	"	-
23	62.5	9.94	15.43	"	"	-	-140+200	"	"	"	-
24	60.6	13.61	22.02	"	"	1 $CaCl_2$	-65+100	"	"	"	-
25	68.2	17.80	22.02	"	"	"	"	"	"	"	-
26	54.9	9.94	12.59	"	"	4 $CaCl_2$	"	"	"	"	-
27	58.7	11.54	16.78	"	"	"	"	"	"	"	-
28	58.7	5.24	9.43	"	"	2 $CaCl_2$	"	"	"	"	-

...Contd.

Table (Contd.)

1	2	3	4	5	6	7	8	9	10	11	12
29	45.5	7.35	10.48	600	60/40	2 $CaCl_2$	-65+100	H_2-H_2O	10	Air	-
30	75.8	5.24	7.35	"	"	1 $CaCl_2$	"	"	"	"	-
31	60.6	13.65	18.35	"	"	"	"	"	"	"	-
32	62.5	7.35	11.03	"	"	0.5 $CaCl_2$	"	"	"	"	-
33	45.5	1.57	2.62	"	"	"	"	"	"	"	-
34	47.4	2.08	4.19	"	"	-	"	"	"	"	-
35	68.2	9.43	12.05	"	"	-	"	"	"	"	-
36	62.5	30.43	35.64	"	"	4 $MgCl_2$	"	"	"	"	-
37	62.5	28.14	34.98	"	"	"	"	"	"	"	-
38	47.4	13.50	17.47	"	"	2 $MgCl_2$	"	"	"	"	-
39	51.1	2.24	4.50	"	"	"	"	"	"	"	-
40	37.9	2.24	4.50	"	"	"	"	"	"	"	-
41	37.9	2.37	2.96	"	"	"	"	"	"	"	-
42	49.2	5.35	7.11	"	"	1 $MgCl_2$	"	"	"	"	-
43	41.1	4.74	5.93	"	"	"	"	"	"	"	-
44	70.0	9.39	11.60	"	70/30	-	"	"	"	"	150°(7hr)
45	70.0	8.28	12.15	"	"	-	"	"	"	"	"

...Contd.

Table (Contd.)

1	2	3	4	5	6	7	8	9	10	11	12
46	70.0	8.85	10.48	600	85/15	-	-65+100	H_2-H_2O	10	Air	150°C (7hr.)
47	70.0	13.80	16.02	"	"	-	"	"	"	"	"
48	58.7	1.42	3.86	"	50/50	-	"	"	"	"	"
49	58.7	1.42	3.37	"	"	-	"	"	"	"	"
50	70.0	15.47	20.97	"	85/15	-	"	"	"	"	-
51	70.0	15.47	22.10	"	"	-	"	"	"	"	-
52	70.0	8.26	11.03	"	60/40	-	"	"	"	"	250°C (7hr)
53	72.0	8.85	12.16	"	"	-	"	"	"	"	"
54	70.0	4.99	6.62	"	"	-	"	"	"	"	-
55	70.0	6.08	8.30	"	"	-	"	"	"	"	-
56	64.4	6.35	8.30	"	"	-	"	"	"	"	-
57	60.6	7.75	11.04	"	"	-	"	"	"	"	-
58	74.0	3.87	4.42	"	"	-	"	N_2	60	"	-
59	77.3	3.31	5.52	"	"	-	"	"	"	"	-
60	3.8	0.55	1.10	"	"	-	"	Air	60	"	-
61	3.8	0.55	1.10	"	"	-	"	"	"	"	-
62	7.6	4.42	4.97	700	"	-	"	N_2	"	"	-

...Contd.

Table (Contd.)

1	2	3	4	5	6	7	8	9	10	11	12
63	3.8	1.66	4.42	700	60/40	-	-85+100	N_2	60	Air	-
64	72.0	8.83	13.81	"	"	-	"	"	75	"	-
65	3.8	0.55	1.66	"	"	-	"	Air	60	"	-
66	3.8	0.55	1.93	600	"	-	"	(H_2+H_2O) $+N_2$	300+ 720	"	-
67	3.8	0.55	2.48	"	"	-	"	"	"	"	-
68	10.0	0.55	2.20	"	"	-	"	H_2-H_2O	60	"	-
69	4.6	0.55	3.86	"	"	-	"	"	"	"	-
70	0.0	0.55	1.93	"	"	-	"	"	960	"	-
71	5.3	0.55	2.20	"	"	-	"	"	"	"	-
72	45.5	1.10	2.76	"	"	-	"	-	0	"	-
73	45.5	1.10	2.48	"	"	-	"	-	0	"	-
74	73.5	30.94	35.67	700	"	-	"	-	0	"	-
75	72.0	28.72	37.56	"	"	-	"	-	0	"	-
76	72.0	27.06	32.58	800	"	-	"	-	0	"	-
77	49.2	2.21	4.42	600	"	-	"	H_2-H_2O	5	"	-
78	87.1	19.92	23.75	800	"	-	"	"	1200	"	-

Conversion factor, Ni % x 0.66 = Ni, ppm.; Fe % x 27.47 = Fe, ppm.

REFERENCES

1. Lapham, D.M., 'A new nickeliferous magnesium hydroxide from Laccaster country, Pennsylvania', Am. Mineralogists, 50(10), 1965, pp 1708-16.

2. Combes, P.J., 'A propos in nickel dens les laterites nickeliferous de la Nonvelle-Caledonie', Comp. Rend. Acad. Sci., 256, 1963, pp 211-12.

3. Turner, A.R. 'The distribution and association of nickel in the ferreginoses zones of the Laterites of the Gyiles Complex, Amdell. Bull. 5, 1968, pp 76-93.

4. Roorda, H.J. and Queneau, P.E., 'Recovery of nickel and cobalt from Limonites by aqueous chlorination in sea water', Trans. IMM, 82, 1973, pp C79-C87.

5. Machpherson, H.G. and Livongstone, A. 'Nickel hydroxides from Unst. Shetland', Min. Mag., 39, 1974, pp 718-20.

6. Panda, S.C., Dey, D.N., Rao, P.K. and Jena, P.K., 'Extraction of nickel and cobalt from lateritic ores of Orissa by pressure leaching with sulphuric acid', Trans. IIM, 28(6), 1975, pp 483-87.

7. Canterford, J.H., 'The Extractive Metallurgy of Nickel', Review Pure and Appl. Chem., 22, 1972, pp 13-46.

8. Webber, B.N. 'Supergene Nickel deposits', Trans AIME, 252, 1972, pp 333-47.

9. Roy, S., Chakravorty, D.C., Murthy, K.K., Bulick, B.B. and Hore, T.B., 'A note on the nickel mineralisation in the Sukinda valley, Cuttack District, Orissa', Indian Minerals, 27(1), 1973, p. 48.

10. Kar, P., Datta, N.R. and Roy S., 'Nickel mineralisation in the Sukinda Ultramafic field, Cuttack District, Orissa', Indian Minerals, 27, 1973, p. 29.

11. Inouye, K., Ichimura, K., Kameko, K. and Ishikawa, T., 'The effect of copper(II) on the formation of γ-FeOOH', Corr. Sci., 16, 1976, pp 507-17.

12. Pigeaud, A., 'The kinetics of nickel passivation', J. Electrochem. Soc., 122(1), 1975, pp 80-83.

13. Boldt, J.R. and Queneau, P.E., 'The winning of Nickel', D. Van Nostrand Co. Inc., Princeton, N.J., 1967.

14. Carlson, E.T. and Simons, C.S., 'Acid leaching Moa Bay's nickel', J. Metals, 12(3), 1960, pp 206-13.

15. Rice, N.M. and Strong, L.W., 'Leaching of laterite nickel ores in hydrochloric acids', Can. Metall., Q13(3), 1974, pp 485-493.

16. Siedel, D.C. and Fitzhugh, E.F., 'A hydrothermal process for oxidised nickel ores', Trans. SME-AIME, 241, 1968, pp 261-268.

17. Fitzhugh, E.F. and Siedel, D.C., 'Nickel cementation', Trans. SME-AIME, 238, 1967, pp 380-386.

18. Queneau, P.E. and Roorda, H.J. 'Impressive new process uses chlorine and seawater for improved recovery of cobalt from nickeliferous Limonites', Mining Eng. 23(8), 1971, pp 70-73.

19. Apostolidis, C.I. and Distin, P.A., 'The kinetics of the sulphuric acid leaching of nickel and magnesium from reduction roasted serpentine', Hydrometallurgy, 3, 1978, pp 181-196.

20. Siemens, R.E. and Corrick, J.D., 'Process for recovery of nickel, cobalt and copper from domestic laterites', Mining Congress Journal, 63(1), 1977, pp. 29-34.

21. Barbery, G., Libande, J., Morizot, G. and Ollivier, P. 'Sulphidation of nickel oxide ores (with high magnesium content), Proceedings of XII IMPC, Brazil, 1977, pp 3-32.

22. Siemens, R.E., Good, P.C. and Stickney, W.A. 'Recovery of nickel and cobalt from low-grade domestic laterites', U.S.B.M. Report No. 8027, 1975, pp 1-13.

23. Siemens, R.E., Stickney, W.A. and Wells, R.R. 'Recovery of nickel and cobalt from low-grade laterites', Proceedings XIth IMPC, Italy, 1975, pp 229-242.

24. Tavares, J.R.P. and Ferreira, R.C.H. 'Recovery of nickel from laterites by reduction with high sulphur mineral coal and tailings from coal concentration plants', Proceedings XII IMPC, Brazil, 1977, pp 3-22.

25. Caron, M.H. 'Fundamental and Practical Factors in Ammonia Leaching of Nickel and Cobalt Ores', Trans AIME, J. Metals, 188, 1950, pp 67-90.

26. Distin, P.A., Nickel extraction from reduction-roasted laterite ores by copper sulphate leaching', J. Metals, Nov. 1978, pp 30-35.

27. Power, L.F. and Geiger, G.H. 'The application of the reduction roast-ammoniacal ammonium carbonate leach to nickel laterites', Mineral Sci. Engg., 9(1), 1977, pp 32-51.

28. Shea, J.F. and Tangel, O.F. 'Large scale laboratory investigation of the ammonium sulphate leaching-hydrogen reduction process as applied to Nicaro bulk precipitates, Trans. AIME, 217, 1960, pp 221-229.

29. Sherritt Gordon Mines Ltd. 'Leaching process for reduced nickel and cobalt bearing laterite ores', British Patent 1182,207, Feb. 1970.

30. Stevens, L.G., Goeller, L.A. and Miller, M. 'Hydrometallurgical recovery of nickel values from laterites', U.S. Patent 3903241, Sept. 1975.

31. O'Neill, C.E. 'Acid extraction of nickel from Lateritic Ores', U.S. Patent 3773891, Oct. 1972.

32. Sherritt Gordon Mines Ltd., Canadian Patent 748374, Dec. 1966.

33. Sherritt Gordon Mines Ltd., British Patent 1064248, April 1967.

34. Matsuzuka, K. 'A method of treating nickel-chromium-containing iron ores', British Patent 951063, March 1964.

35. Hedley, N. and Kress, J. 'Treatment of Garnierite Ores', U.S. Patent 2349223, May 1944.

36. Chizhikov, D.M., Karyazina, I.M., Mel'nik, Yu. I. and Kovtim, V.A. 'The reduction of ferrous metals from an oxidised nickel ore with hydrogen and methane', Russ. Met., 6, 1975, pp 18-21.

37. Chizhikov, D.M., Tzvetkov, Yu. V., Karyazina, I.N., Kovtim, V.A. and Blokhina, L.I. 'Kinetics of Garnierite reduction with hydrogen and Methane', Russ Met. 5, 1972, pp 36-39.

38. German Patents 1245400, Aug. 1968 and 1263316, Sept. 1968; French Patent 1470580, March 1967; British Patent 1080210, Aug. 1967. (These have been taken from pp 42-43 of Ref. 7 above.)

39. Kulp, J.L. and Trites, A.F. 'DTA of natural hydrous ferric oxide', Amer. Min., 36, 1951, pp 23-44.

40. Francombe, M.H. and Rooksby, H.P. 'Structure transformations effected by the dehydration of diaspore, Goethite and γ-Fe_2O_3, Clay. Min. Bull., 4, 1959, pp 1-14.

41. Mackenzie, R.C. (Ed.), 'The DTA investigation of Clays', Mineralogical Society, London, 1957, Chapter 12.

42. Thiel, R. 'Zum system α-FeOOH-α-AlOOH, Z. Anorg. Allg. Chem., 326, 1963, pp 70-78.

43. Kelly, W.C. 'Application of DTA to identification of the natural hydrous ferric oxides', Am. Min., 41, 1956, pp 353-5.

44. Smykatz-Kloss, W., 'Differential Thermal Analysis - Application and results in mineralogy', Springer-Verlag, Berlin, Heidelberg, New York, 1974, pp. 36,39,92.

45. Carver, J.C., Schweitzer, G.K. and Carlson, T.A., 'Use of X-ray photoelectron spectroscopy to study bonding in Cr, Mn, Fe and Co compounds', J. Chem. Phys. 57(2), 1972, pp 973-82.

46. Allen, G.C., Curtis, M.T., Hooper, A.J. and Tucker, P.M., 'X-ray photoelectronscopy of iron-oxygen systems', J. Chem. Soc., Dalton, 1974, Part 2, p. 1525.

47. Gimzewski, J.K., Padalia, B.D. and Affrossman, S., 'The reaction of oxygen and water with iron films Studied by X-ray Photoelectron Spectroscopy', Surface Science, 62, 1977, pp 386.

48. Kishi, K. and Ikeda, S. 'X-ray photoelectron spectroscopic study for the reaction of evaporated iron with O_2 and H_2O', Bull. Chem. Soc., Japan, 46, 1973, pp 341-345.

49. Wheeler, D.R. and Brainard, W.A. 'X-ray photoelectron spectroscopy study of radio frequency-sputtered refractory-compound-steel interfaces', NASA Technical Paper 1161, 1968, p. 12.

50. Stucki, J.W., Roth, C.B. and Baitinger, W.E., 'Analysis of iron-bearing clay minerals by electron spectroscopy for chemical analysis' (ESCA), Clays and Clay Minerals, 24, 1976, p 289.

Date Slip

This book is to be returned on the date last stamped.

.....	.....
.....	.....
.....	.....
.....	.....
.....	.....
.....	.....
.....	.....
.....	.....
.....	.....
.....	.....
.....	.....

CD 6.72.9